

Journal of Taibah University for Science

ISSN: (Print) 1658-3655 (Online) Journal homepage: http://www.tandfonline.com/loi/tusc20

Soret and Dufour effects on heat and mass transfer in chemically reacting MHD flow through a wavy channel

J.A. Gbadeyan, T.L. Oyekunle, P.F. Fasogbon & J.U. Abubakar

To cite this article: J.A. Gbadeyan, T.L. Oyekunle, P.F. Fasogbon & J.U. Abubakar (2018) Soret and Dufour effects on heat and mass transfer in chemically reacting MHD flow through a wavy channel, Journal of Taibah University for Science, 12:5, 631-651, DOI: 10.1080/16583655.2018.1492221

To link to this article: https://doi.org/10.1080/16583655.2018.1492221

© 2018 The Author(s). Published by Informa UK Limited, trading as Taylor & Francis Group

Published online: 09 Jul 2018.

Submit your article to this journal

Article views: 100

View Crossmark data

Full Terms & Conditions of access and use can be found at
http://www.tandfonline.com/action/journalInformation?journalCode=tusc20

JOURNAL OF TAIBAH UNIVERSITY FOR SCIENCE
2018, VOL. 12, NO. 5, 631–651
https://doi.org/10.1080/16583655.2018.1492221

OPEN ACCESS Check for updates

Soret and Dufour effects on heat and mass transfer in chemically reacting MHD flow through a wavy channel

J.A. Gbadeyan [a], T.L. Oyekunle[c], P.F. Fasogbon [b] and J.U. Abubakar [a]

[a]Department of Mathematics, University of Ilorin, Ilorin, Nigeria; [b]Department of Mathematics, Obafemi Awolowo University, Ile-Ife, Nigeria; [c]Department of Mathematics, College of Education, Oro, Nigeria

ABSTRACT

The problem of coupled heat and mass transfer by free convection of a chemically reacting viscous incompressible and electrically conducting fluid confined in a vertical channel bounded by wavy wall and flat wall in the presence of diffusion-thermo (Dufour), thermal-diffusion (Soret) and internal heat source or sink is studied. The walls are maintained at constant but different temperatures and species concentrations. A uniform magnetic field β_0 is acting transversely to the walls which are assumed to be electrically non-conducting. The dimensionless governing equations are perturbed into mean part (zeroth-order) and perturbed part (first-order), using amplitude as a perturbation parameter. The first-order quantities are obtained by long wave approximation. The resulting set of coupled ordinary differential equations are solved numerically using the Adomian decomposition method. Some of the results indicating the influence of various parameters on the zeroth-order and first-order fluid flow, heat and mass transfer characteristics are presented graphically.

ARTICLE HISTORY
Received 8 July 2017
Accepted 10 November 2017

KEYWORDS
Chemical reaction; magneto-hydrodynamic; free convection; wavy channel; Adomian decomposition method

1. Introduction

Recently, there has been some renewed attentions in the study of free convective heat and mass transfer in fluid flow through a wavy or irregular channel. This is because the analysis of such flows find applications in various industrial and engineering problems such as nuclear reactor, heat ex-changers, transpiration cooling of re-entry vehicles and rocket boosters, film vapourization in combustion chambers and cross-hatching on ablative surfaces [1,2]. Additional significant applications include the use of rough (wavy) walls in medical apparatus to increase the mass transfer in blood (blood oxygenator). Rough surfaces are often used as flow passages in several applications for controlling the rate of heat transfer, cooling of electronic components and the designing of ventilating-heating building [3,4].

Some of the mentioned studies include, for example, the work of Vajraelu and Sastri [1] who examined the influence of waviness of one of the walls on the flow and heat transfer characteristics of an incompressible viscous fluid confined between two long vertical walls. Fasogbon [2] discussed analytically, the studies of heat and mass transfer by free convection in a two-dimensional irregular channel. Recently, the effects of chemical reaction and heat source on two-dimensional free convection magneto-hydrodynamics (MHD) flow in an irregular channel with porous medium were investigated by Davika et al. [3]. Most recently, two-dimensional heat transfer of a free convection MHD flow with radiation and temperature-dependent heat source of a viscous incompressible fluid in a porous medium within a wavy channel were discussed by Dada and Disu [4]. Fasogbon and Omolehin [5] examined the radiation effect on natural convection in an irregular channel. Abubakar [6] studied the effect of the wall slip on a laminar two-dimensional free convective flow of fluid confined between an irregular wall and a flat wall. He discovered that increase in the slip parameter at the flat wall leads to a decrease in fluid velocity. Kumar [7] studied two-dimensional heat transfer of a free convective MHD flow with radiation and temperature-dependent heat source of a viscous incompressible fluid in a vertical irregular channel.

Meanwhile, it is well known that for a simultaneous occurrence of heat and mass transfer in a moving fluid, the relationships between the driven potential and the corresponding fluxes are of important. Also it is noticed that the energy flux (rate of energy transfer per unit area) and mass flux (rate of mass flow per unit area) can be generated by temperature gradients as well as composition gradients. The energy caused or generated by composition gradients is known as Dufour or diffusion-thermo effect and is considered useful in isotope separation. The mass flux created or generated by temperature gradients is known as Soret or thermal-diffusion effect which is consid-

CONTACT T.L. Oyekunle tloyekunle95@gmail.com

© 2018 The Author(s). Published by Informa UK Limited, trading as Taylor & Francis Group
This is an Open Access article distributed under the terms of the Creative Commons Attribution License (http://creativecommons.org/licenses/by/4.0/), which permits unrestricted use, distribution, and reproduction in any medium, provided the original work is properly cited.

ered useful in mixture of gases with very light molecular weight (hydrogen–helium) and medium molecular weight (nitrogen–air) Kafoussias and William [8]. In view of the technological important applications of Soret and Dufour effects in sciences and engineering, these terms are considered in energy and concentration equations respectively in the present work.

In view of these applications, Gbadeyan et al. [9] examined the effects of thermal-diffusion and diffusion-thermo on combined heat and mass transfer on mixed convective boundary layer flow over a stretching vertical surface in a porous medium filled with a viscoelastic fluid in the presence of magnetic field. Makinde and Olanrewaju [10] carried out the study of an unstable mixed convection with Soret and Dufour effects past a porous plate moving through a binary mixture of chemically reacting fluid. Olanrewaju and Gbadeyan [11] analysed a mathematical model in order to study the effect of Soret, Dufour, chemical reaction, thermal radiation and volumetric heat generation/absorption on mixed convection stagnation point flow on an isothermal vertical plate in a porous media. Alam et al. [12] studied Dufour and Soret effects on steady free convection and mass transfer flow past a semi-infinite vertical porous plate in a porous medium. Olanrewaju et al. [13] analysed the influence of chemical reaction, thermal radiation, thermal-diffusion, diffusion-thermo on hydromagnetic free convection with heat and mass transfer past a vertical plate with suction/injection. Also, Olanrewaju and Makinde [14] investigated free convective heat and mass transfer of an incompressible electrically conducting fluid past a moving vertical plate in the presence of suction and injection with thermal-diffusion (Soret) and diffusion-thermo (Dufour) effects.

MHD (magneto fluid dynamics or hydromagnetics) is the study of the dynamics of electrically conducting fluids. Example of such fluid include plasma, liquid metal and salt water or electrolytes.The fundamental concept behind MHD is that magnetic field can induce electrical currents in a moving conductive fluid, which in turn creates forces on the fluid and also changes the magnetic field itself, this has led to extensive studies of MHD fluid flow. For example, Das and Ahmed [15] studied the problem of free convective MHD flow and heat transfer in a viscous incompressible fluid confined between a long wavy wall and a parallel flat wall. Disu and Dada [16] examined two-dimensional heat transfer of a free convective-radiative MHD flows with variable viscosity and heat source of a viscous incompressible fluid in a porous medium between two vertical wavy walls.

Also chemical reaction is a process that leads to transformation of one set of chemical substances to another. The chemical reactions are central to chemical engineering where they are used for synthesis of new compound from natural raw materials such as petroleum, mineral ores and thermite reaction to generate light and heat in pyrotechnics and welding. The presence of a foreign mass in air or water causes some kind of chemical reaction. Some foreign mass may be present either naturally or mixed with air or water. It is enormous practical consequence to engineers and scientists, because of the study of heat and mass transfer with chemical reaction is almost universal occurrence in many branches of science and engineering (Loganathan et al. [17]). In this article [17], the authors examined the influence of chemical reaction on unsteady free convective and mass transfer flow past a vertical plate with variable viscous and thermal conductivity. Also, the natural convective power-law fluid flow past a vertical plate embedded in a non-darcian porous medium in the presence of a homogeneous chemical reaction is studied in Chamka et al. [18].

Furthermore, heat transfer is a process by which internal energy from one substance transfers to another and mass transfer is the transport of a substance (mass) in liquid or gaseous media. Heat and mass transfer occur simultaneously in many processes, such as drying evaporation at the surface of the wet body, energy transfer in a wet cooling tower, flow in a desert cooler, polymer production and food processing. In view of these applications, therefore, it is of interest to combine heat and mass transfer with chemical reaction, MHD, Dufour and Soret effects because of their applications in many processes occurring both in nature and industries involving fluid flow.

However, to the best of our knowledge, no work has been done on the problem of free convection heat and mass transfer in a viscous fluid flowing over a wavy wall or confined between two walls one or both of which are wavy, involving chemical reaction in the presence of both Soret and Dufour. Thus, there is a definite need for the investigation of such a problem. This fact along with the potential application of this problem represent the significance of the present work. Hence, the goal of the present work is, therefore, to investigate the combined effects of Soret and Dufour on heat and mass transfer in chemically reacting MHD flow through a rough (wavy) channel. The non-dimensional coupled boundary value problem governing the fluid flow was perturbed and the resulting zeroth- and first-order boundary value problem were solved using the Adomian decomposition method with MAPLE 14 software.

2. Formulation of the research problem

The channel considered is made up of a finitely long irregular (wavy) wall at one end and a flat wall at the other. The X'-axis is taken to be vertically upward and parallel to the flat wall in the direction of bouyancy, while Y'-axis is perpendicular to the X'-axis in such a way that the position of irregular wall is represented by $Y' = \epsilon^* \cos kX'$, $|\epsilon^*| < 1$, and that of the flat wall is represented by $Y' = d$ (Figure 1).

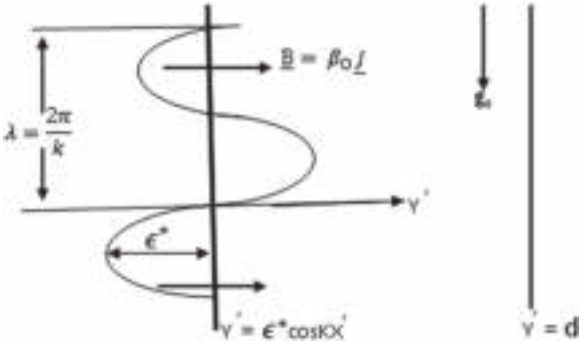

Figure 1. The flow channel.

In formulating this problem, the following assumptions are made:

(I) The irregular and flat walls are at constant temperatures T_w and T_1, respectively and constant concentrations C_w and C_1, respectively.
(II) All fluid properties are constant except the density in the bouyancy force term.
(III) The viscous and magnetic dissipation are neglected in the energy equation and that work done by pressure are sufficiently small in comparison with both the flow by conduction, wall temperatures and wall concentrations.
(IV) The flow is laminar, steady, hydromagnetic and two-dimensional.
(V) The volumetric heat source/sink term in energy equation is constant and the small amplitude wall roughness is characterized by a certain wavelength $\lambda = (2\pi/k)$, where k is the wave number.
(VI) The thermal-diffusion and diffusion-thermo are of substantial magnitudes such that they cannot be neglected.
(VII) The electric field is assumed to be zero, the induced magnetic field is negligible compared to the applied magnetic field, since the magnetic Reynolds number is very small for most fluid used in industrial application.
(VIII) The reaction is of first-order, the rate of reaction is directional proportional to concentration differences.

Based on these assumptions with the usual Boussinesq approximation, the governing equations of steady two-dimensional heat and mass transfer are made up of the following dimensional continuity, momentum, energy and species equations.

Continuity equation

$$\frac{\partial U'}{\partial X'} + \frac{\partial V'}{\partial Y'} = 0. \tag{1}$$

Momentum equations

$$\rho\left(U'\frac{\partial U'}{\partial X'} + V'\frac{\partial U'}{\partial Y'}\right) = -\frac{\partial P'}{\partial X'} + \mu\left(\frac{\partial^2 U'}{\partial X'^2} + \frac{\partial^2 U'}{\partial Y'^2}\right) - \rho g_x - \sigma\beta_0^2 U', \tag{2}$$

$$\rho\left(U'\frac{\partial V'}{\partial X'} + V'\frac{\partial V'}{\partial Y'}\right) = -\frac{\partial P'}{\partial Y'} + \mu\left(\frac{\partial^2 V'}{\partial X'^2} + \frac{\partial^2 V'}{\partial Y'^2}\right). \tag{3}$$

Energy equation

$$\rho C_P\left(U'\frac{\partial T'}{\partial X'} + V'\frac{\partial T'}{\partial Y'}\right) = K\left(\frac{\partial^2 T'}{\partial X'^2} + \frac{\partial^2 T'}{\partial Y'^2}\right) + Q + \frac{\rho D_m K_T}{C_s}\left(\frac{\partial^2 C'}{\partial X'^2} + \frac{\partial^2 C'}{\partial Y'^2}\right), \tag{4}$$

and Concentration equation

$$\left(U'\frac{\partial C'}{\partial X'} + V'\frac{\partial C'}{\partial Y'}\right) = D_m\left(\frac{\partial^2 C'}{\partial X'^2} + \frac{\partial^2 C'}{\partial Y'^2}\right) + \frac{D_m K_T}{T_m}\left(\frac{\partial^2 T'}{\partial X'^2} + \frac{\partial^2 T'}{\partial Y'^2}\right) - k_1(C' - C_s'). \tag{5}$$

The corresponding boundary conditions of the problem are taken as

$$U' = 0, \quad V' = 0, \quad T' = T_w, \quad C' = C_w \text{ on } Y' = \epsilon^* \cos kX', \tag{6}$$

$$U' = 0, \quad V' = 0, \quad T' = T_1, \quad C' = C_1 \text{on } Y' = d. \tag{7}$$

Furthermore, it is remarked at this juncture, that for free convection flows, the associated velocities are considerably small while the presence of viscous energy dissipation term usually calls for high-speed flows. Hence, the above assumption that the influence of the viscous dissipation term in the energy equation may be considered negligible is practically reasonable, on the other hand, the inclusion of Joule heating's (magnetic dissipation) effect is of importance for fluid whose medium possesses very high electrical conductivity. However, fluid whose medium is of low electrical conductivity are considered in this problem. Hence, the effect of the magnetic dissipation may be safely regarded negligible. Similar argument hold for the above assumptions.

The following non-dimensional variables

$$\begin{aligned} (x, y) &= \frac{1}{d}(X', Y'), \quad (u, v) = \frac{d}{\nu}(U', V'), \\ \lambda &= kd, \quad \epsilon = \frac{\epsilon^*}{d}, \quad p = \frac{P' d^2}{\rho \nu^2}, \\ p_s &= \frac{P_s' d^2}{\rho \nu^2}, \quad \theta = \frac{T - T_s}{T_w - T_s}, \quad T_s \neq T_w, \\ c &= \frac{C' - C_s'}{C_w - C_s'}, \quad C_s' \neq C_w \end{aligned} \tag{8}$$

were introduced into equations (1)–(7) to obtain the following non-dimensional equations.

Continuity equation

$$\frac{\partial u}{\partial x}+\frac{\partial v}{\partial y}=0. \tag{9}$$

Momentum equations

$$u\frac{\partial u}{\partial x}+v\frac{\partial u}{\partial y}=-\frac{\partial p}{\partial x}+\frac{\partial^2 u}{\partial x^2}+\frac{\partial^2 u}{\partial y^2}-\frac{g_x d^3}{\nu^2}-Hu, \tag{10}$$

$$u\frac{\partial v}{\partial x}+v\frac{\partial v}{\partial y}=-\frac{\partial p}{\partial y}+\frac{\partial^2 v}{\partial x^2}+\frac{\partial^2 v}{\partial y^2}. \tag{11}$$

Energy equation

$$P_r\left(u\frac{\partial \theta}{\partial x}+v\frac{\partial \theta}{\partial y}\right)=\frac{\partial^2\theta}{\partial x^2}+\frac{\partial^2\theta}{\partial y^2}+p_rD_u\left(\frac{\partial^2 c}{\partial x^2}+\frac{\partial^2 c}{\partial y^2}\right)+\alpha, \tag{12}$$

and Concentration equation

$$S_c\left(u\frac{\partial c}{\partial x}+v\frac{\partial c}{\partial y}\right)=\frac{\partial^2 c}{\partial x^2}+\frac{\partial^2 c}{\partial y^2}+S_cS_r\left(\frac{\partial^2\theta}{\partial x^2}+\frac{\partial^2\theta}{\partial y^2}\right)-S_c\gamma c. \tag{13}$$

The corresponding boundary conditions are

$$u=v=0,\quad \theta=c=1 \text{ on } y=\epsilon\cos\lambda x, \tag{14}$$

$$u=v=0,\quad \theta=m1,\quad c=m2 \text{ on } y=1, \tag{15}$$

In the static fluid (subscripts), we have

$$0=\frac{\partial P_s}{\partial x}-\frac{\rho_s g_x d^3}{\rho\nu^2}, \tag{16}$$

so that equation (10) becomes

$$u\frac{\partial u}{\partial x}+v\frac{\partial u}{\partial y}=-\frac{\partial(p-p_s)}{\partial x}+\frac{\partial^2 u}{\partial x^2}+\frac{\partial^2 u}{\partial y^2}+G1\theta_1+G2c_1-Hu, \tag{17}$$

$\rho_s=\rho\{1+\beta_T(T_w-T_s)\theta+\beta_c(C_w-C_s')c\}$ is the well-known Boussinesq approximation.

where

$$G1=\frac{d^3g_x\beta_T(T_w-T_s)}{\nu^2},\quad G2=\frac{d^3g_x\beta_c(C_w-C_s')}{\nu^2},$$
$$H=\frac{d^2\sigma\beta_0}{\rho\nu},P_r=\frac{\mu C_p}{K},\quad \alpha=\frac{Qd^2}{K(T_w-T_s)},$$
$$S_c=\frac{\nu}{D_m},\quad D_u=\frac{D_mK_T(C_w-C_s')}{C_sC_pK(T_w-T_s)},$$
$$S_r=\frac{D_mK_T(T_w-T_s)}{\nu T_m(C_w-C_s')},\quad \gamma=\frac{k_1d^2}{\nu},$$
$$m1=\frac{T_1-T_s}{T_w-T_s},\quad m2=\frac{C_1-C_s'}{C_w-C_s'}. \tag{18}$$

All the physical variables are as defined in the nomenclature.

3. Method of solution

The irregularity of the wall is assumed small, hence, it is appropriate to seek a perturbation solution for small ϵ. The limit $\epsilon=0$ is, of course, the limit of a smooth flat wall, for which the solution is well known. Thus we take the flow field variables, velocity, pressure, temperature and concentration as

$$\left.\begin{aligned}u(x,y)=u_0(y)+\epsilon u_1(x,y),\, v(x,y)=\epsilon v_1(x,y),\\ p(x,y)=p_0(x)+\epsilon p_1(x,y),\\ \theta(x,y)=\theta_0(y)+\epsilon\theta_1(x,y)\\ c(x,y)=c_0(y)+\epsilon c_1(x,y).\end{aligned}\right\} \tag{19}$$

Putting equation (19) into equations (9)–(13), we obtained zeroth- and first-order set of equations where the perturbed quantities u_1, v_1, θ_1 and c_1 are small compared with mean or the zeroth-order quantities u_0, θ_0 and c_0.

For zeroth-order (by equating the coefficients of ϵ^0), we have

$$\frac{d^2u_0}{dy^2}+G1\theta_0+G2c_0-Hu_0=c_p, \tag{20}$$

$$\frac{d^2\theta_0}{dy^2}+P_rD_u\frac{d^2c_0}{dy^2}=-\alpha, \tag{21}$$

$$\frac{d^2c_0}{dy^2}+S_cS_r\frac{d^2\theta_0}{dy^2}-S_c\gamma c_0=0, \tag{22}$$

with the following boundary conditions

$$\begin{aligned}&u_0=0,\quad \theta_0=c_0=1 \text{ on } y=0,\\ &u_0=0,\ \theta_0=m1,\ c_0=m2 \text{ on } y=1,\end{aligned} \tag{23}$$

where $c_p=(\partial(p_0-p_s)/\partial x)$, and is taken to be equal to zero, following [1,2].

And for first-order (by equating coefficients of ϵ^1), we have

$$\frac{\partial u_1}{\partial x}+\frac{\partial v_1}{\partial y}=0, \tag{24}$$

$$u_0\frac{\partial u_1}{\partial x}+v_1\frac{du_0}{dy}=-\frac{\partial p_1}{\partial x}+\frac{\partial^2 u_1}{\partial x^2}+\frac{\partial^2 u_1}{\partial y^2}+G1\theta_1+G2c_1-Hu_1, \tag{25}$$

$$u_0\frac{\partial v_1}{\partial x}=-\frac{\partial p_1}{\partial y}+\frac{\partial^2 v_1}{\partial x^2}+\frac{\partial^2 v_1}{\partial y^2}, \tag{26}$$

$$P_r\left(u_0\frac{\partial\theta_1}{\partial x}+v_1\frac{d\theta_0}{dy}\right)=\frac{\partial^2\theta_1}{\partial x^2}+\frac{\partial^2\theta_1}{\partial y^2}+P_rD_u\left(\frac{\partial^2 c_1}{\partial x^2}+\frac{\partial^2 c_1}{\partial y^2}\right), \tag{27}$$

$$S_c\left(u_0\frac{\partial c_1}{\partial x}+v_1\frac{dc_0}{dy}\right) = \frac{\partial^2 c_1}{\partial x^2}+\frac{\partial^2 c_1}{\partial y^2}+S_cS_r\left(\frac{\partial^2\theta_1}{\partial x^2}+\frac{\partial^2\theta_1}{\partial y^2}\right)-S_c\gamma c_1, \tag{28}$$

with the boundary conditions

$$\left.\begin{aligned} u_1=-u_0',\quad v_1=0,\quad \theta_1=-\theta_0', c_1=-c_0' \text{ on } y=0,\\ u_1=0,\quad v_1=0,\quad \theta_1=0,\quad c_1=0 \text{ on } y=1,\end{aligned}\right\} \tag{29}$$

where prime denotes differentiation with respect to Y. To solve equations (24)–(29), we introduce stream function $\psi_1(x,y)$ defined as

$$u_1=-\frac{\partial\psi_1(x,y)}{\partial y},\quad v_1=\frac{\partial\psi_1(x,y)}{\partial x}. \tag{30}$$

So that (24) is satisfied and eliminating the dimensionless pressure p_1, we obtain

$$\frac{\partial^4\psi_1}{\partial y^4}+\frac{\partial^4\psi_1}{\partial x^4}+2\frac{\partial^4\psi_1}{\partial x^2\partial y^2}-u_0\frac{\partial^3\psi_1}{\partial x\partial y^2}-u_0\frac{\partial^2\psi_1}{\partial x^3} + \frac{d^2u_0}{dy^2}\frac{\partial\psi_1}{\partial x}-H\frac{\partial^2\psi_1}{\partial y^2}=G1\frac{\partial\theta_1}{\partial y}+G2\frac{\partial c_1}{\partial y}, \tag{31}$$

$$P_r\left(u_0\frac{\partial\theta_1}{\partial x}+\frac{d\theta_0}{dy}\frac{\partial\psi_1}{\partial x}\right)=\frac{\partial^2\theta_1}{\partial x^2}+\frac{\partial^2\theta_1}{\partial y^2} + P_rD_u\left(\frac{\partial^2 c_1}{\partial x^2}+\frac{\partial^2 c_1}{\partial y^2}\right), \tag{32}$$

$$S_c(u_0\frac{\partial c_1}{\partial x}+\frac{dc_0}{dy}\frac{\partial\psi_1}{\partial x})=\frac{\partial^2 c_1}{\partial x^2}+\frac{\partial^2 c_1}{\partial y^2} + S_cS_r(\frac{\partial^2\theta_1}{\partial x^2}+\frac{\partial^2\theta_1}{\partial y^2})-S_c\gamma c_1, \tag{33}$$

while the corresponding boundary conditions become

$$\left.\begin{aligned} \frac{\partial\psi_1}{\partial y}=u_0',\quad \frac{\partial\psi_1}{\partial x}=0,\quad \theta_1=-\theta_0',\\ c_1=-c_0' \text{ on } y=0,\\ \frac{\partial\psi_1}{\partial x}=0,\quad \frac{\partial\psi_1}{\partial x}=0,\quad \theta_1=0,\\ c_1=0 \text{ on } y=1.\end{aligned}\right\} \tag{34}$$

Due to the nature of the wall, we assume wave-like solutions of the form

$$\psi_1(x,y)=\epsilon\ell^{i\lambda x}\psi(\lambda,y),\quad \theta_1(x,y)=\epsilon\ell^{i\lambda x}\phi(\lambda,y),\quad c_1(x,y)=\epsilon\ell^{i\lambda x}\varphi(\lambda,y), \tag{35}$$

perturbation series expansion for small wavelength in which terms of exponential order arise from which we deduce that

$$u_1(x,y)=-\epsilon e^{i\lambda x}\psi(\lambda,y),\quad v_1(x,y)=\epsilon i\lambda e^{i\lambda x}\psi(\lambda,y),$$

where i is the complex unit (see [2]).

Substituting (35) into (31)–(34), we have

$$\psi^{''v}-H\psi^{''}=i\lambda(u_0\psi^{''}-\lambda^2u_0\psi-u_0''\psi) + \lambda^2(2\psi^{''}-\lambda^2\psi)+G1\phi'+G2\varphi', \tag{36}$$

$$\phi^{''}=ip_r\lambda(u_0\phi+\theta_0'\psi)+\lambda^2\phi+P_rD_u(\lambda^2\varphi-\varphi^{''}), \tag{37}$$

$$\varphi^{''}=iS_c\lambda(u_0\varphi+c_0'\psi)+(\lambda^2+S_c\gamma)\varphi+S_cS_r(\lambda^2\phi-\phi^{''}), \tag{38}$$

with the boundary conditions

$$\left.\begin{aligned} \psi'=u_0',\quad \psi=0,\quad \theta_1=-\theta_0',\quad c_1=-c_0' \text{ on } y=0,\\ \psi'=0,\quad \psi=0,\quad \theta_1=0,\quad c_1=0 \text{ on } y=1.\end{aligned}\right\} \tag{39}$$

By considering series expansion for small λ (or $k<<1$) of the form

$$\psi(\lambda,y)=\sum_{j=0}^{\infty}\lambda^j\psi_j,\quad \phi(\lambda,y)=\sum_{j=0}^{\infty}\lambda^j\phi_j, \quad \varphi(\lambda,y)=\sum_{j=0}^{\infty}\lambda^j\varphi_j\ (j=0,1,2\ldots), \tag{40}$$

putting (40) into equations (36)– (39) on restriction to the real parts of the solutions for the perturbed quantities and retaining up to order λ^2, we obtained the following sets of differential equations.

$$O(\lambda^0):\quad \psi_0^{''v}-H\psi_0^{''}=G1\phi_0'+G2\varphi_0',\quad \phi_0^{''}=-P_rD_u\varphi_0^{''},\quad \varphi_0^{''}=S_c\gamma\varphi_0-S_cS_r\phi_0^{''}, \tag{41}$$

$$\left.\begin{aligned} O(\lambda):\quad \psi_1^{''v}-H\psi_1^{''}=i(u_0\psi_0^{''}-u_0^{''}\psi_0)+G1\phi_1'+G2\varphi_1',\\ \phi_1^{''}=ip_r(u_0\phi_0+\theta_0'\psi_0)-P_rD_u\varphi_1^{''},\\ \varphi_1^{''}=iS_c(u_0\varphi_0+c_0'\psi_0)+S_c\gamma\varphi_1-S_cS_r\phi_1^{''},\end{aligned}\right\} \tag{42}$$

$$\left.\begin{aligned} O(\lambda^2):\quad \psi_2^{''v}-H\psi_2^{''}=i(u_0\psi_1^{''}-u_0^{''}\psi_1)\\ +2\psi_0^{''}+G1\phi_2'+G2\varphi_2',\\ \phi_2^{''}=ip_r(u_0\phi_1\\ +\theta_0'\psi_1)+\phi_0+P_rD_u(\varphi_0-\varphi_2^{''}),\\ \varphi_2^{''}=iS_c(u_0\varphi_1+c_0'\psi_1)\\ +\varphi_0+S_c\gamma\varphi_2+S_cS_r(\phi_0-\phi_2^{''}),\end{aligned}\right\} \tag{43}$$

with the corresponding boundary conditions

$$\left.\begin{aligned} \psi_0'=u_0',\quad \psi_0=0,\quad \phi_0=-\theta_0',\quad \varphi_0=-c_0' \text{ on } y=0,\\ \psi_0'=0,\quad \psi_0=0,\quad \phi_0=0,\quad \varphi_0=0 \text{ on } y=1,\end{aligned}\right\} \tag{44}$$

$$\left.\begin{aligned} \psi_j'=0,\quad \psi_j=0,\quad \phi_j=0,\quad \varphi_0=0 \text{ on } y=0\\ \psi_j'=0,\quad \psi_j=0,\quad \phi_j=0,\quad \varphi_j=0 \text{ on } y=1\end{aligned}\right\} \forall j\geq 1. \tag{45}$$

The zeroth-order problems, made up of equations (20)–(22) with boundary condition (23) and the first-order

problems, made up of equations (41)–(43) with the boundary conditions (44) and (45) are solved, using the Adomian decomposition method programme written by [19] with MAPLE 14 software and obtained the expression for (u_0, θ_0 and c_0) and (u_1, v_1, θ_1 and c_1) as the zeroth-order and first-order solutions, respectively, where λx is taken to be $(\pi/2)$ following [2]. The solutions are not presented here for the sake of brevity.

4. Discussion of the zeroth-order and first-order results

The primary objective of this paper is to investigate the effects of Soret S_r, Dufour D_u and chemical reaction γ on heat and mass transfer by free convection flow through a wavy/irregular channel under the influence of an externally applied magnetic field and heat source/sink. This objective is accomplished by evaluating numerically, the expressions for the zeroth-order and the first-order velocity, temperature and concentration. The solutions are presented through graphs.

In the numerical discussion that follows, for physical reality, we take Prandtl number to be 0.71 which corresponds to the air at 20^0C. Schmidt number is chosen to represent the presence of diffusing chemical species of most common interest in air, e.g. carbon dioxide CO_2 at 25^0C at one atmosphere pressure ($S_c = 1.0$). The values of $(G1, G2)$ take positive value, which corresponds to cooling the wall or heating the fluid by free convection currents. The parameter α and $(m1, m2)$ are varied to stimulate physically realistic situations. α is the heat sink $(\alpha < 0 = -5)$/source $(\alpha > 0 = 5)$. In the absence of heat source, we have $\alpha = 0$. Physically, $m1$,$m2 = -1$ means that the temperatures and concentrations of the two walls are equal to that of the static fluid while $m1$,$m2 = 2$ means equal wall temperatures and concentrations. In the absence of chemical reaction, we have $\gamma = 0$ while $\gamma < 0$ corresponds to exothermic chemical reaction and $\gamma > 0$ corresponds to endothermic chemical reaction. The geometric parameters representing the waviness/roughness of the wall (the amplitude ϵ, the wavelength λ and λx). The amplitude $\epsilon > 0 = 0.25$, characteristic of dilated channel and $\lambda x = \pi/2$ have been fixed while $\lambda = 0.001, 0.002$ is varied. The values of the other parameters are chosen arbitrarily.

4.1. Discussion of the zeroth-order results

4.1.1. Velocity profiles

In order to get a clear insight of the physical problem, the velocity, temperature and concentration profiles have been discussed by assigning numerical values to various parameters encountered in the problem. The results are presented graphically and conclusions are drawn for the flow field and other physical quantities of interest that have significant effects. To test the validity of our results, a comparison of the present results with those of the previous works [1,2] are performed by setting the introduced new parameters (i.e D_u, S_r, H, $G2$ and γ) to zero and excellent agreements were obtained (see Figures 2 and 3).

The zeroth-order velocity (u_0) profiles when $m1 = -1$ are plotted against y in Figure 2. It is observed that in the presence of heat source $(\alpha > 0)$ with an increase in the free convection parameter $G1$, the velocity u_0 increases across the entire channel width (curves III and VI). When there is heat sink $(\alpha < 0)$ and the free convection parameter $G1$ increases, the velocity (u_0) decreases across the entire channel width (curves I and IV). In the absence of heat generation or absorption $(\alpha = 0)$, the fluid velocity increases in the first half of the channel width $(y = 0.5)$ and then decreases with an increase in the free convection parameter $G1$ (curves II and V). However, when the heat source parameter α increases with constant free convection parameter $G1$, the velocity u_0 increases considerably (curves I, II, III) and (curves IV, V, VI).

Figure 3 depicts the zeroth-order velocity u_0 profile when $m1 = 2$. It is noticed that the fluid velocity u_0 increases generally as the free convection parameter $G1$ increases for all the value of heat generation parameter α (curves I and IV, II and V, III and VI). On fixing the

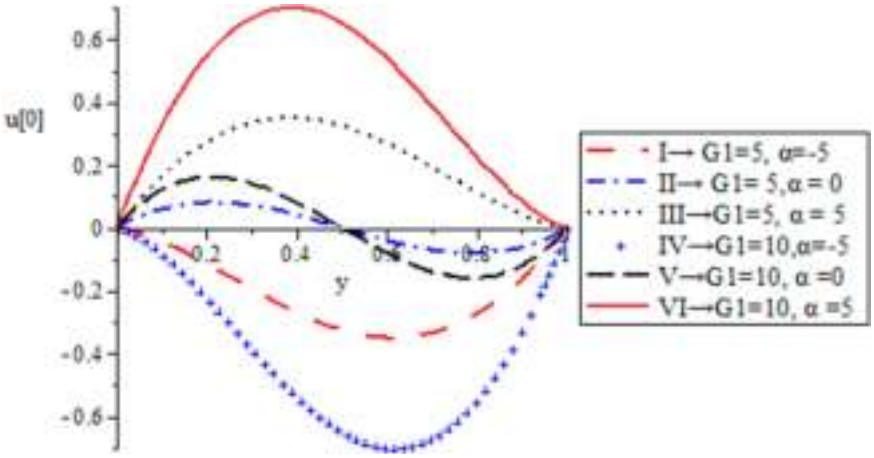

Figure 2. Zeroth-order velocity u_0 profile, $m1 = -1, m2 = 0, D_u = 0, S_r = 0, H = 0, G2 = 0, \gamma = 0, P_r = 0.71$ and $S_c = 0.60$.

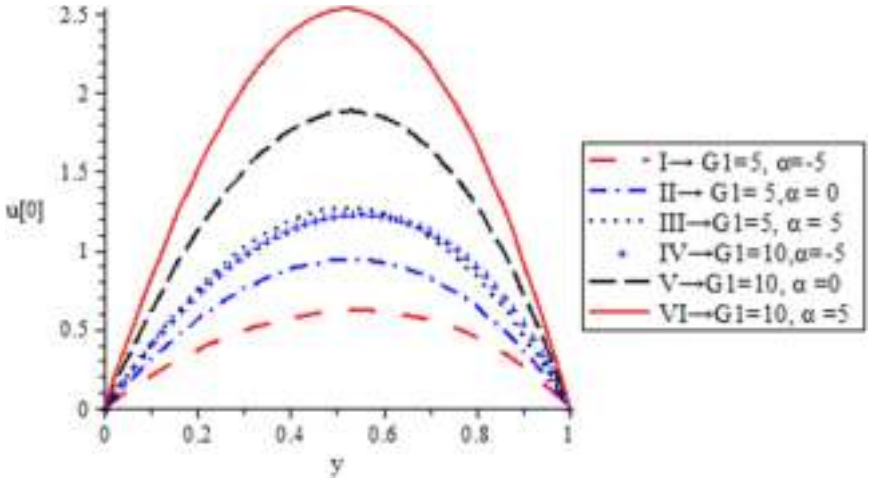

Figure 3. Zeroth-order velocity u_0 profile, $m1 = 2, m2 = 0, D_u = 0, S_r = 0, H = 0, G2 = 0, P_r = 0.71, S_c = 0.60$ and $\gamma = 0$.

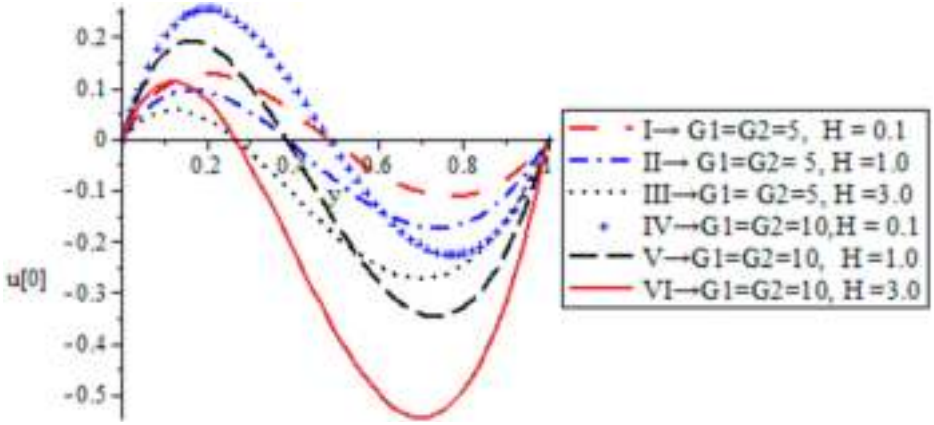

Figure 4. Zeroth-order velocity u_0 profile, $m1 = m2 = -1, \gamma = 4, S_r = 2.0, \alpha = -5, P_r = 0.71, S_c = 0.60$ and $D_u = 0.60$.

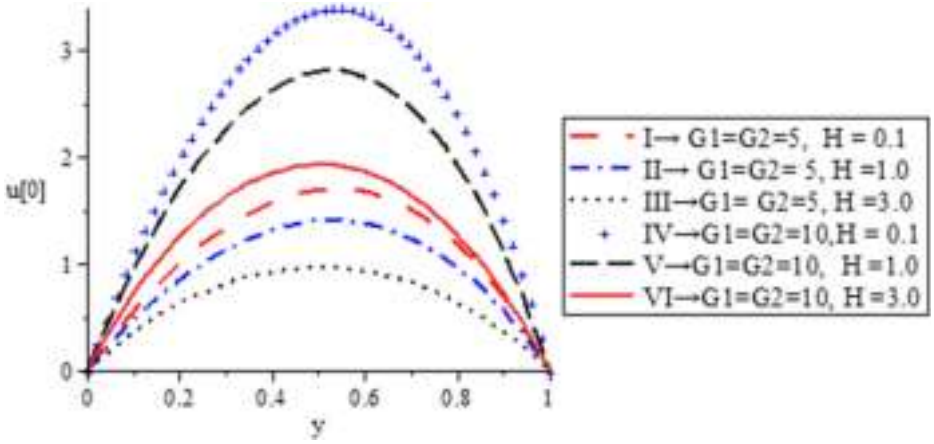

Figure 5. Zeroth-order velocity u_0 profile, $m1 = m2 = 2, \gamma = 4, S_r = 2.0, \alpha = -5, P_r = 0.71, S_c = 0.60$ and $D_u = 0.60$.

free convection parameter $G1$ and increasing the heat source parameter α, it is found that the velocity (u_0) also increases across the channel width (curves I, II and III) and (curves IV, V and VI).

Figure 4 shows the effect of MHD (H) on the fluid flow when $m1 = m2 = -1$. It is clearly seen that when there is an increase in H with constant free convection parameters $G1$and $G2$, the velocity u_0 decreases across the entire channel width (curves I, II, III) and (curves IV, V, VI). When the free convection parameters $G1$ and $G2$ increase with a fixed magnetic parameter $H = 0.1$, the velocity increases to a certain point $y = 0.5$ on the channel width and then decreases (curves I and IV). For $H = 1$ and $H = 3$, the velocity increases up to $y = 0.4$ (curves II and V) and $y = 0.28$ (curves III and VI), respectively, and then decreases.

Figure 5 represents the effects of magnetic field (H) when $m1 = m2 = 2$. It is observed that an increase in H with constant free convection parameters $G1$ and $G2$ leads to a decrease in velocity u_0 (curves I, II, III) and

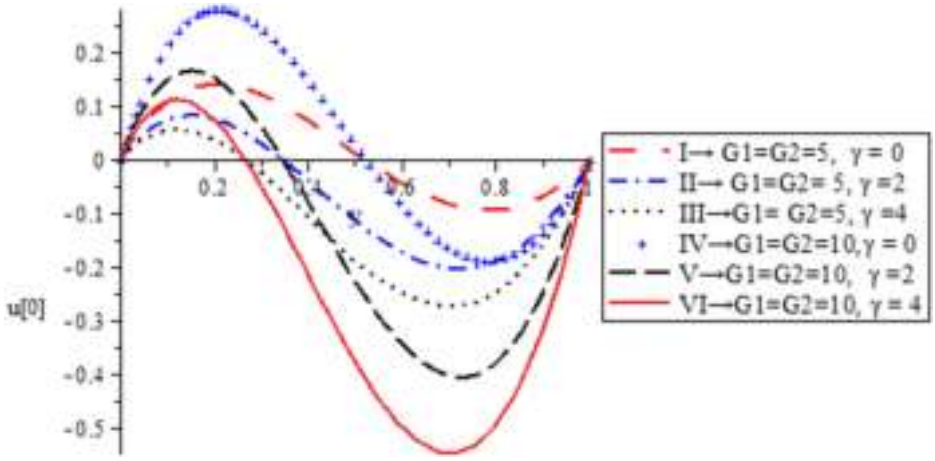

Figure 6. Zeroth-order velocity u_0 profile, $m1 = m2 = -1$, $\alpha = -5$, $S_r = 2.0$, $H = 3.0$, $P_r = 0.71$, $S_c = 0.60$ and $D_u = 0.60$.

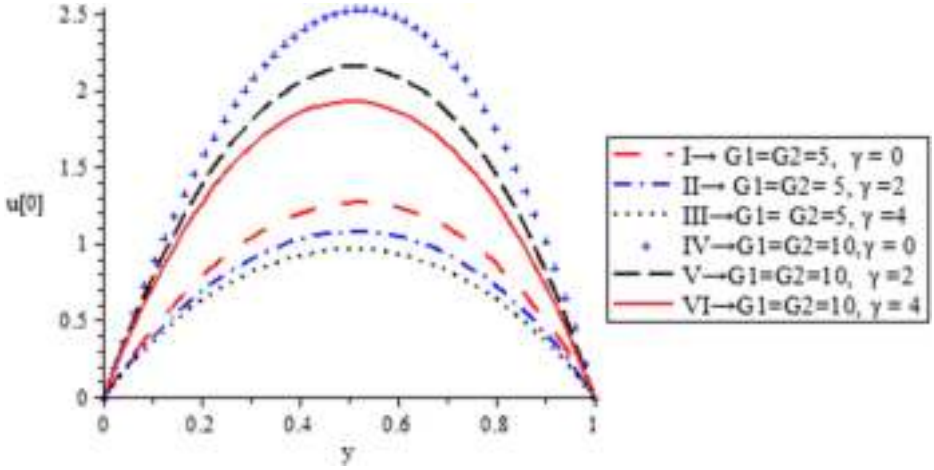

Figure 7. Zeroth-order velocity u_0 profile, $m1 = m2 = 2$, $\alpha = -5$, $S_r = 2.0$, $H = 3.0$, $P_r = 0.71$, $S_c = 0.60$ and $D_u = 0.60$.

(curves IV, V, VI). We also noticed that for an increase in free convection parameters $G1$ and $G2$ with a fixed magnetic parameter H, the velocity u_0 increases (curves I and IV, II and V, III and VI).

The effects of chemical reaction (γ) is presented in Figure 6 for $m1 = m2 = -1$. It is clearly seen that an increase in γ with a fixed free convection parameters $G1$ and $G2$ leads to a decrease in velocity (u_0) profile (curves I, II, III) and (curves IV, V, VI). An increase in $G1$ and $G2$ with a fixed chemical reaction parameter, leads to an increase in the velocity (u_0) profile to a particular point on the width of the channel and then decreases (curves I and IV, II and V, III and VI).

For $m1 = m2 = 2$. Figure 7 described the effects of chemical reaction on the velocity(u_0) profiles. It is observed that when the free convection parameters $G1$ and $G2$ are fixed, the velocity u_0 decreases with an increase in chemical reaction parameter γ (curves I, II, III) and (curves IV, V, VI). Also, when free convection parameter increases the velocity increases with constant chemical reaction parameter (curves I and IV, II and V, III and VI).

Figure 8, when $m1 = m2 = -1$, shows that an increase in Dufour parameter D_u with constant free convection parameters leads to a decrease in velocity profile (curves I, II, III) and (curves IV, V, VI). It is also noticed that an increase in free convection parameters with constant Dufour parameter increases the velocity (u_0) profile to a particular point on the channel width and then decreases (curves I and IV, II and V, III and VI).

In Figure 9, when $m1 = m2 = 2$, it is observed that an increase in Dufour parameter with constant free convection parameters decreases the velocity (u_0) profiles (curves I, II, III) and (curves IV, V, VI). Reverse is the case when Dufour parameter is kept constant with an increase in free convection parameters.

It is clearly seen in Figure 10 that the velocity (u_0) profiles increase across the entire channel width with an increase in Soret parameter when the free convection parameter is kept constant for $m1 = m2 = -1$ (curves I, II, III) and (curves IV, V, VI). Reverse is the case when free convection parameters increases with a constant Soret parameter.

For $m1 = m2 = 2$, Figure 11 shows that when the free convection parameters are fixed, the velocity (u_0) profiles increase with an increase in Soret parameter (curves I, II, II) and (curves IV, V, VI). The same behaviour is observed for velocity when there is an increase in free

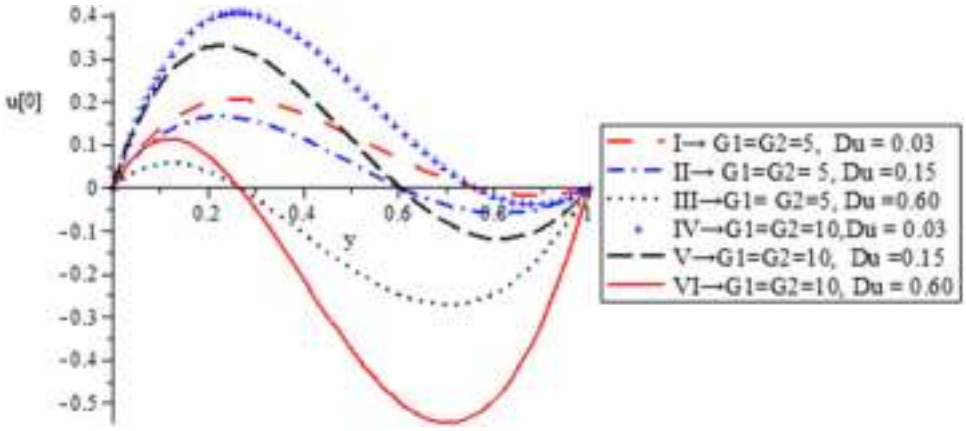

Figure 8. Zeroth-order velocity u_0 profile, $m1 = m2 = -1$, $\alpha = -5$, $S_r = 2.0$, $H = 3.0$, $P_r = 0.71$, $S_c = 0.60$ and $\gamma = 4$.

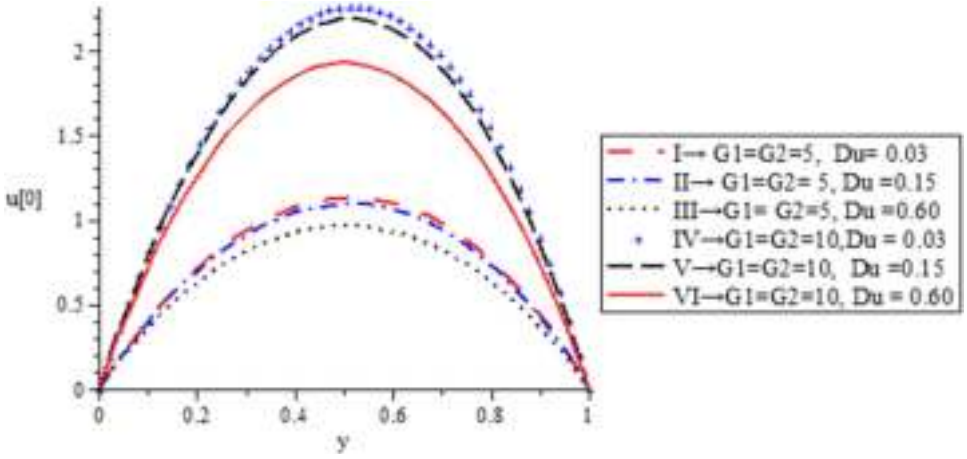

Figure 9. Zeroth-order velocity u_0 profile, $m1 = m2 = 2$, $\alpha = -5$, $S_r = 2.0$, $H = 3.0$, $P_r = 0.71$, $S_c = 0.60$ and $\gamma = 4$.

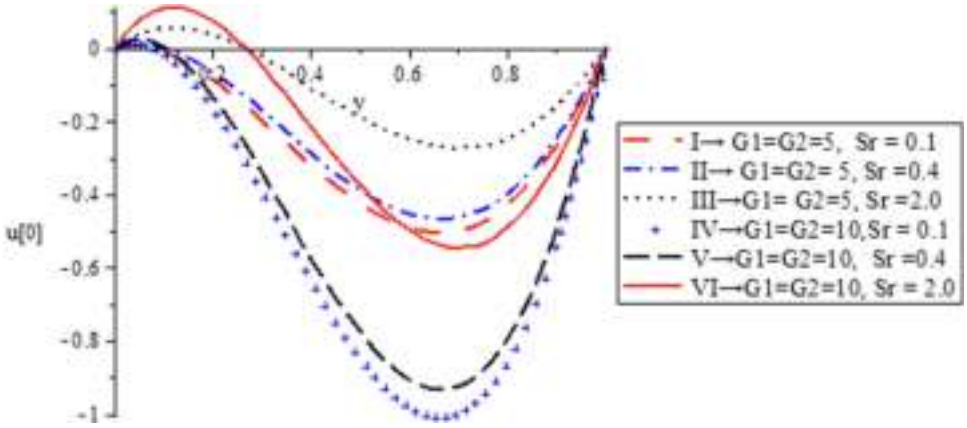

Figure 10. Zeroth-order velocity u_0 profile, $m1 = m2 = -1$, $\alpha = -5$, $D_u = 0.60$, $H = 3.0$, $P_r = 0.71$, $S_c = 0.60$ and $\gamma = 4$.

convection parameters with constant Soret parameter (curves I and IV, II and V, III and VI).

4.1.2. Temperature profiles

As it was done in the discussion on the zeroth-order velocity profiles, we begin our zeroth-order temperature profiles by carrying out a comparison of the present and previous results.

Figure 12 depicts the results of the variation of zeroth-order temperature with y when the new parameters (i.e S_r, D_u, H and γ) are zero. It is seen clearly that when $m1 = -1$, the temperature (θ_0) profiles increase with an increase in heat parameter α. It is also noticed that in the absence of heat sink/source ($\alpha = 0$), the temperature (θ_0) profile is a linearly decreasing function of y while in the presence of heat sink or source it is parabolic in nature. When $m1 = 2$, the temperature (θ_0) profile behaved in the opposite way for all values of heat parameter α.

Figure 13 shows the effects of Soret on the temperature θ_0 profiles. It is clearly seen that an increase in Soret number with constant wall temperature ratios

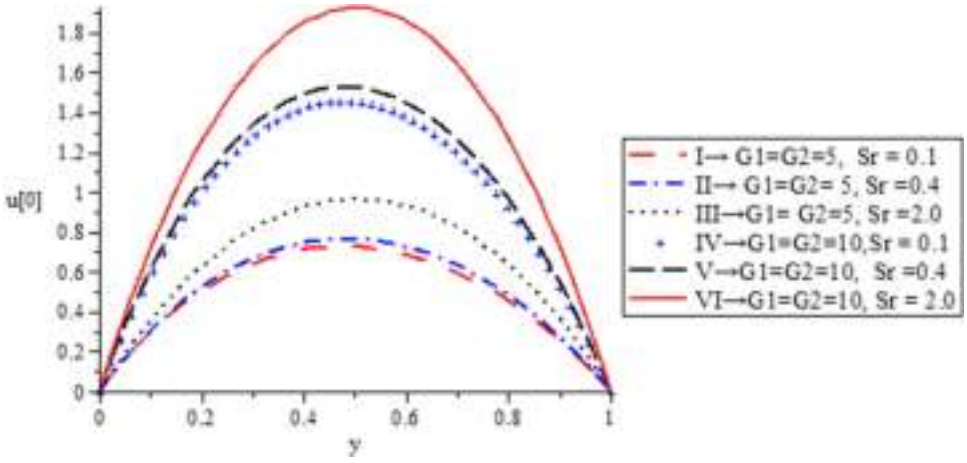

Figure 11. Zeroth-order velocity u_0 profile, $m1 = m2 = 2$, $\alpha = -5$, $H = 3.0$, $P_r = 0.71$, $S_c = 0.60$ and $\gamma = 4$.

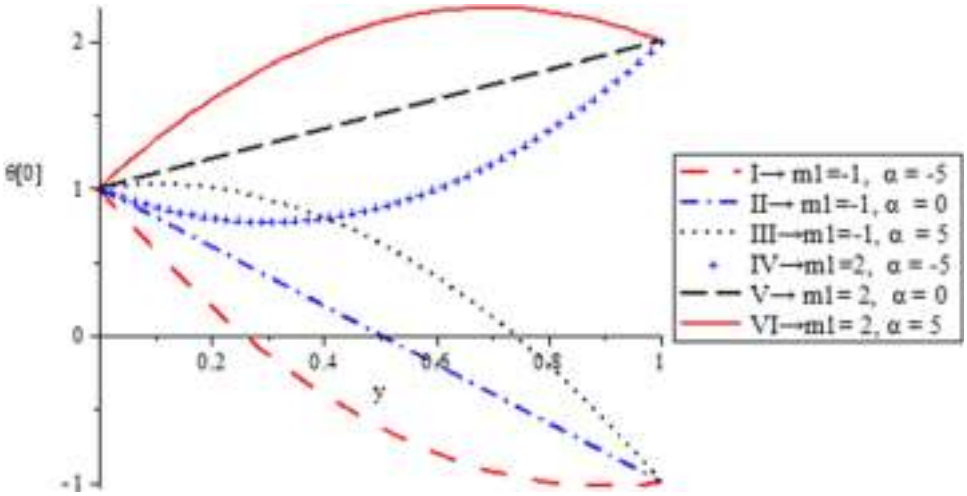

Figure 12. Zeroth-order temperature θ_0 profile, $S_r = 0$, $D_u = 0$, $m2 = 0$, $P_r = 0.71$, $S_c = 0.60$ and $\gamma = 0$.

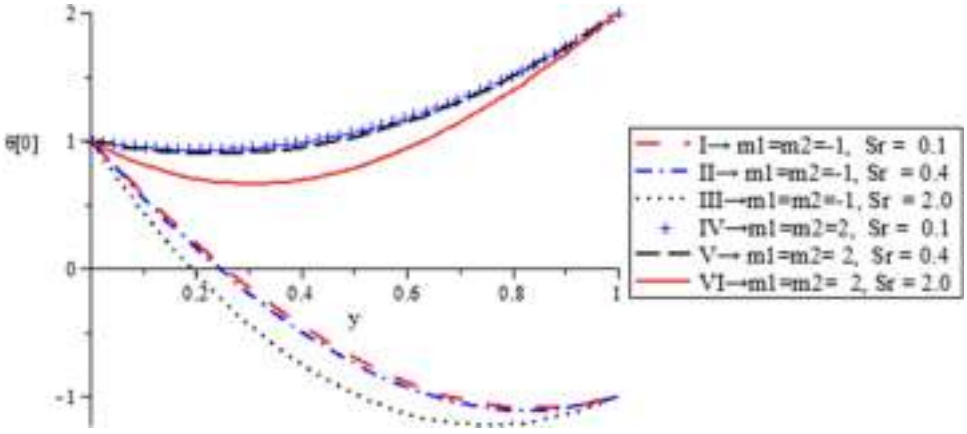

Figure 13. Zeroth-order temperature θ_0 profile, $\alpha = -5$, $D_u = 0.60$, $P_r = 0.71$, $S_c = 0.60$ and $\gamma = 4$.

$(m1 = m2 = -1)$, the temperature θ_0 profiles decrease across the entire channel width (curves I, II, III) and when $m1 = m2 = 2$, the temperature (θ_0) profiles remain the same in behaviour as we have when $m1 = m2 = -1$ (curves IV, V, VI).

Figure 14 deals with the effects of chemical reaction on temperature (θ_0). It is observed that when $m1$ and $m2$ are fixed, temperature (θ_0) profiles increase with an increase in the chemical reaction parameter, γ. In both cases the curves are parabolic in nature (curves I, II, III) and (curves IV, V, VI).

Figure 15 depicts the effects of Dufour, on the temperature θ_0. We noticed that the temperature θ_0 profile increases with an increase in Dufour number D_u. In both cases the curves are parabolic in nature (curves I, II, III) and (curves IV, V, VI).

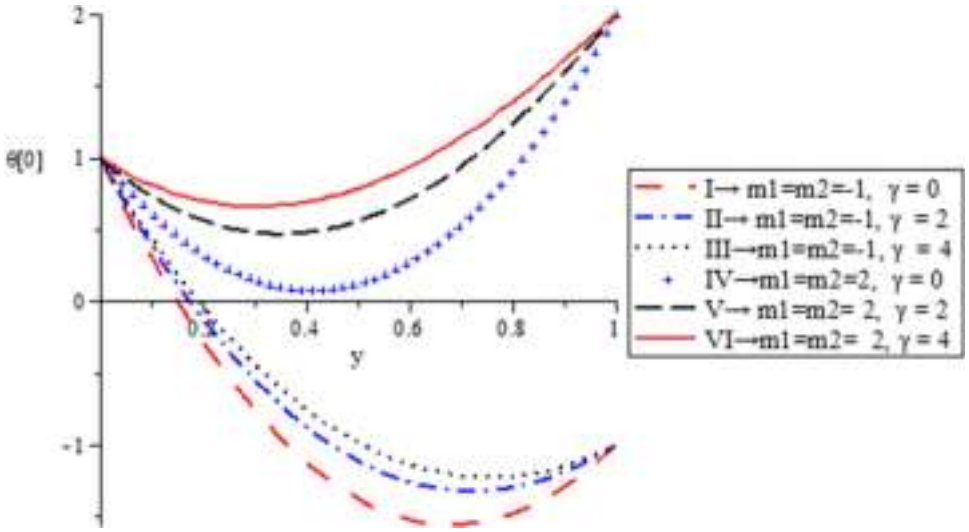

Figure 14. Zeroth-order temperature θ_0 profile, $\alpha = -5$, $D_u = 0.60$, $P_r = 0.71$, $S_c = 0.60$ and $S_r = 2$.

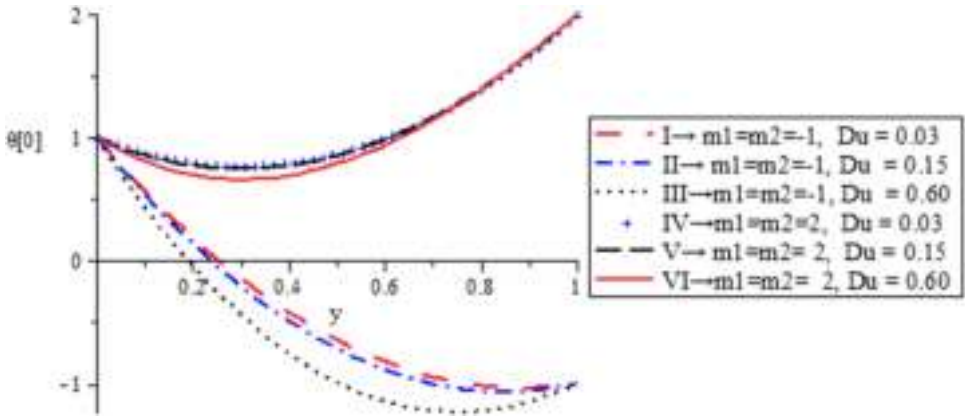

Figure 15. Zeroth-order temperature θ_0 profile, $\alpha = -5$, $\gamma = 4$, $P_r = 0.71$, $S_c = 0.60$ and $S_r = 2$.

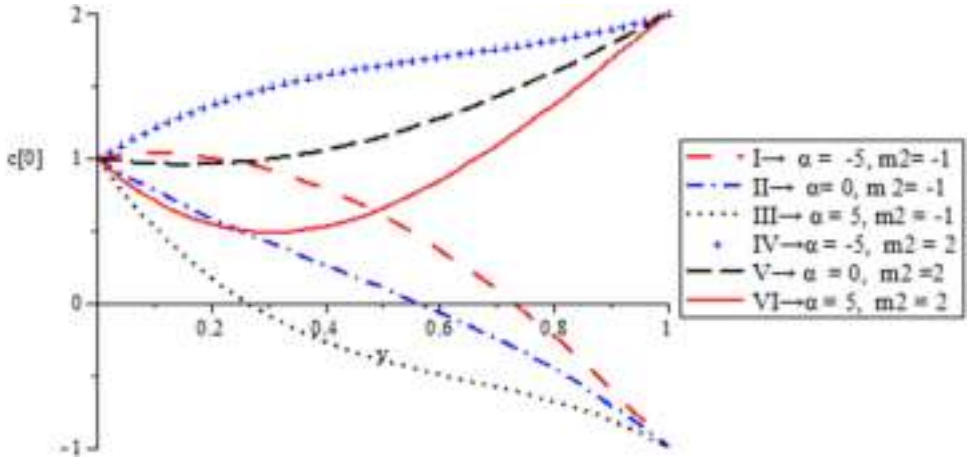

Figure 16. Zeroth-order concentration c_0 profile, $\gamma = 4$, $P_r = 0.71$, $S_c = 0.60$ and $S_r = 2$.

4.1.3. Concentration profiles

Figure 16 shows that on fixing wall concentration ratio $m2 = -1$, the concentration c_0 profiles decrease with an increase in heat source parameter α (curves I, II, III). The concentration profiles behaved the same way as when $m2 = -1$ for $m2 = 2$ with an increase in heat source parameter α (curves IV, V, VI). The curves I, II, III are parabolic functions of y while curves IV, V, VI are parabolic increasing functions of y.

Figure 17 reveals the effects of Soret number on the concentration (c_0) profiles. We noticed that when concentration ratio $m2$ is constant, there is an increase in

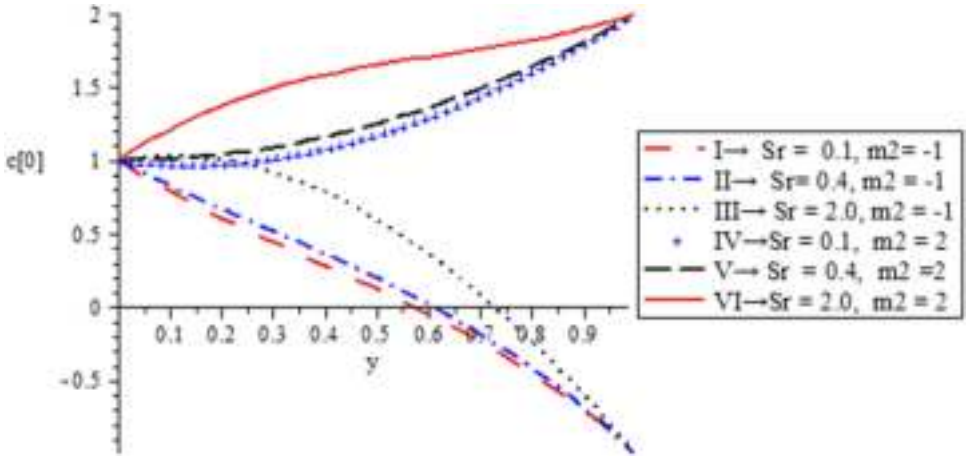

Figure 17. Zeroth-order concentration c_0 profile, $\gamma = 4$, $P_r = 0.71$, $S_c = 0.60$ and $\alpha = -5$.

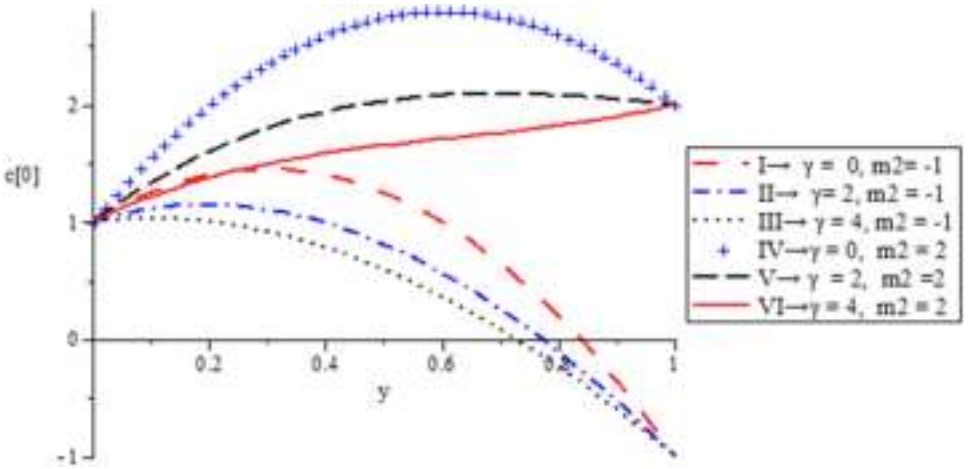

Figure 18. Zeroth-order concentration c_0 profile, $S_r = 2.0$, $P_r = 0.71$, $S_c = 0.60$ and $\alpha = -5$.

concentration (c_0) profiles with an increase in Soret number (curves I, II, III) and (curves IV, V, VI). The curves are parabolic in nature.

Figure 18 shows the effects of chemical reaction (γ) on the concentration (c_0) profiles. It is observed that for a fixed concentration ratio $m2$ and an increase in chemical reaction parameter (γ) leads to a decrease in concentration (c_0) profiles, which are parabolic in nature (curves I, II, III) and (curves IV, V, VI).

4.2. Discussion of the first-order results

4.2.1. Velocity profiles

Figures 19–23 revealed the behaviour of the fluid velocity u (1) profiles along the channel length. Figure 19 presents the behaviour of the perturbed velocity quantity u (1) when $m1 = -1$ and the embedded parameters are set to zero. It is observed that in the presence of heat sinks, the velocity $u(1)$ increases to a particular point of y $(y = 0.5)$ and then decreases with constant free convection parameter $G1$ and frequency parameters λ (curves I and II, VII and VIII). On the other hand, when heat source is considered, there exist an increase in the velocity $u(1)$ up to $y = 0.3$, followed by a decrease up to $y = 0.7$ and finally an increase for $y > 0.7$ (curves II and III, VIII and IX). It is also noticed that with an increase in $G1$ or λ, the velocity increases close to the walls of the channel and decreases in between the walls (curves I and VII, II and VIII, III and IX) or (curves I and IV, II and V, III and VI).

The effect of MHD parameter H on the fluid flow when $m1 = m2 = -1$ is shown in Figure 20. It is clearly seen that when there is an increase in H for constant free convection parameters $G1$,$G2$ and frequency parameters λ, the velocity increases to a point $(y = 0.25)$, decreases to another point $(y = 0.7)$ and then increases (curves I, II, III and VII, VIII, IX). When there is an increase in the frequency λ or free convection $G1$,$G2$ parameters with constant value of H, the velocity increases to certain value of $y(y = 0.25)$ and decreases to $y = 0.70$ and then increases again (curves I and IV, III and VI) or (curves I and VII, III and IX).

Figure 21 shows the effect of Dufour parameter D_u on the fluid flow when $m1 = m2 = -1$. It is observed that with an increase in the Dufour parameter D_u when frequency λ and free convection $G1$,$G2$ parameters are constant, there is an increase in velocity up to $(y = 0.25)$, a decrease up to $(y = 0.7)$ and then an increase. (curves I, II and III) and (curves VII, VIII and IX). It is also noticed that with constant Dufour parameter D_u and an increase in frequency λ or free convection $G1$,$G2$ parameters, the

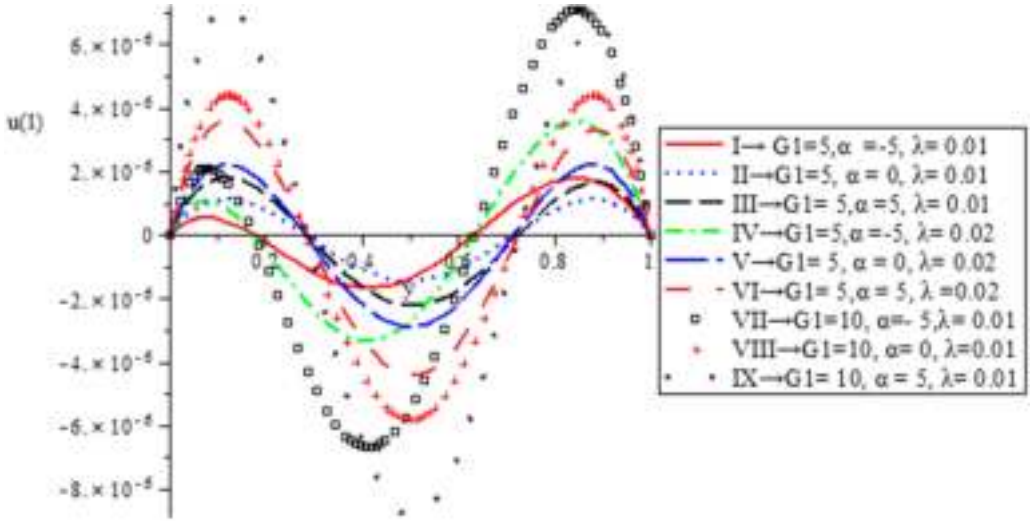

Figure 19. First-order velocity $u(1)$ profile, $m1 = -1$, $P_r = 0.71$, $S_r = 0$, $\gamma = 0$, $S_c = 0$, $D_u = 0$, $G2 = 0$,$m2 = 0$ and $H = 0$.

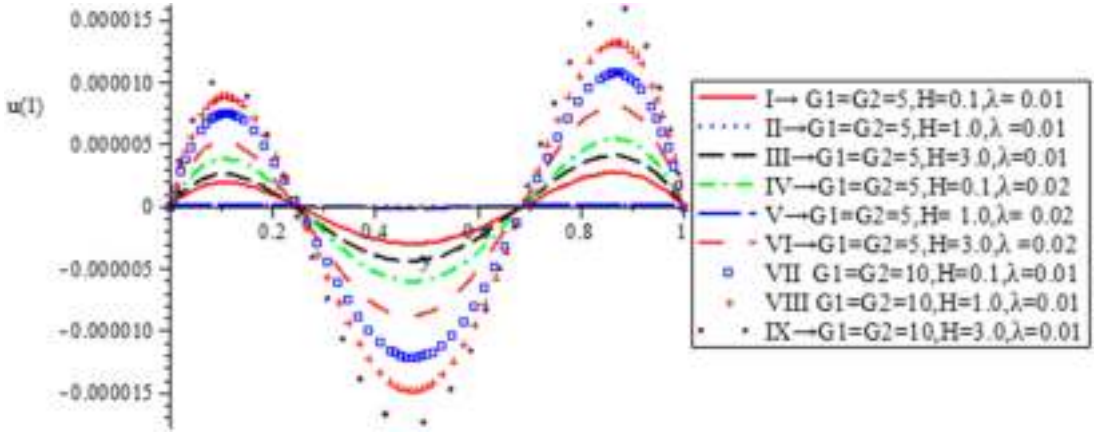

Figure 20. First-order velocity $u(1)$ profile, $m1 = m2 = -1$, $P_r = 0.71$, $S_r = 2$, $\gamma = 4$, $S_c = 0.60$, $D_u = 0.60$ and $\alpha = -5$.

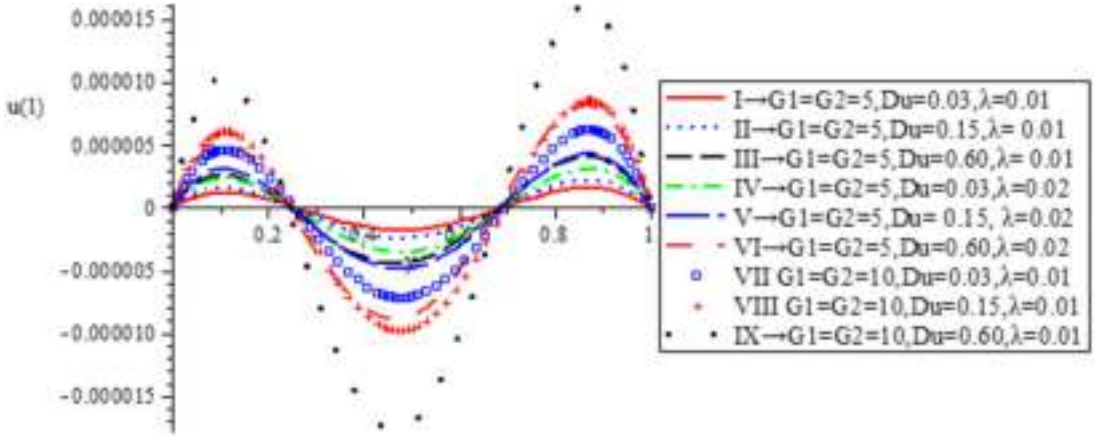

Figure 21. First-order velocity $u(1)$ profile, $m1 = m2 = -1$, $P_r = 0.71$, $S_r = 2$, $\gamma = 4$, $S_c = 0.60$, $H = 3.0$ and $\alpha = -5$.

velocity increases to a particular point $y = 0.25$ on the width of the channel and then decreases to another point $y = 0.7$ after which it increases (curves I and IV, II and V, III and VI) or (curves I and VII, II and VIII, III and IX).

The effect of chemical reaction parameter γ on the fluid flow when $m1 = m2 = -1$ is depicted in Figure 22. It is clearly seen that with an increase in chemical reaction parameter when the frequency λ and free convection $G1$,$G2$ parameters are kept constant, the velocity increases to a particular point $y = 0.25$ and leads to a decrease up to $y = 0.70$ before increasing again along the width of the channel. (curves I, II, III) and (curves VII, VIII IX). It is also observed that with constant chemical reaction parameter γ and an increase in the frequency λ or free convection $G1$,$G2$ parameters, there is an increase in velocity up to $y = 0.25$, a decrease

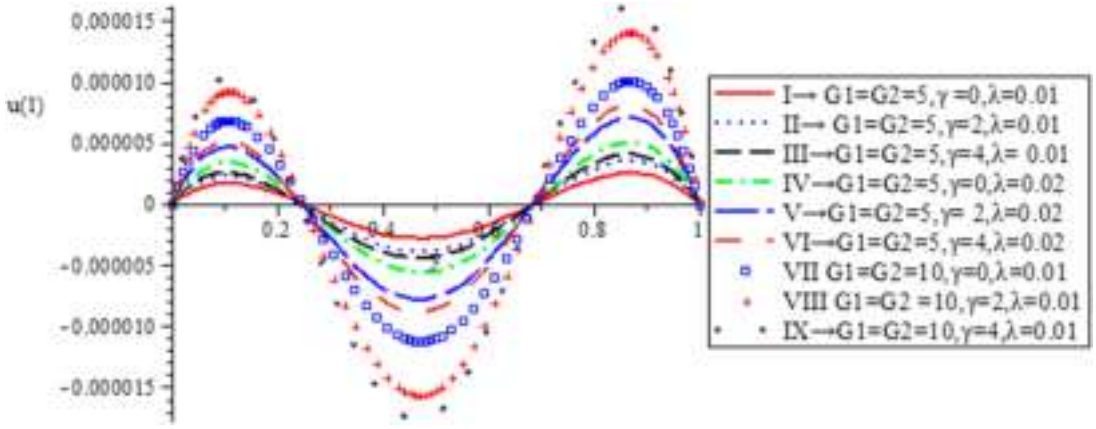

Figure 22. First-order velocity $u(1)$ profile, $m1 = m2 = -1$, $P_r = 0.71$, $S_r = 2$, $D_u = 0.60$, $S_c = 0.60$, $H = 3.0$ and $\alpha = -5$.

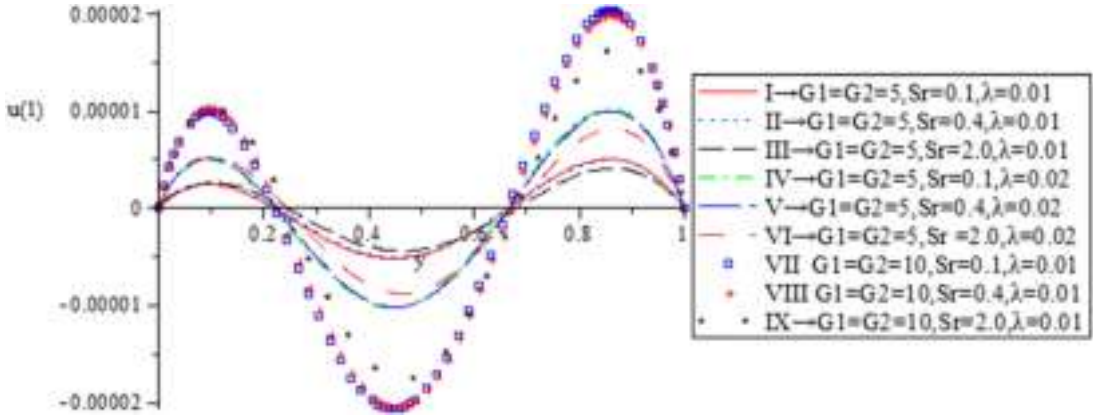

Figure 23. First-order velocity $u(1)$ profile, $m1 = m2 = -1$, $P_r = 0.71$, $\gamma = 4$, $D_u = 0.60$, $S_c = 0.60$, $H = 3.0$ and $\alpha = -5$.

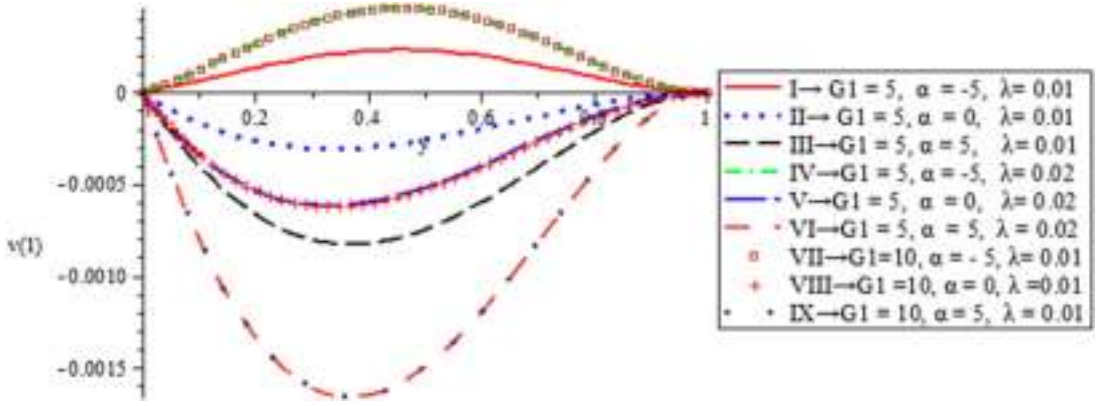

Figure 24. First-order velocity $v(1)$ profile, $m = -1$, $P_r = 0.71$, $S_r = 0$, $\gamma = 0$, $S_c = 0$, $D_u = 0$, $G2 = 0$, $m2 = 0$ and $H = 0$.

between $y = 0.25$ and 0.70 while it then increases along the width of the channel (curves I and IV, II and V, III and VI) or (curves I and VII, II and VIII, III and IX).

Figure 23 describe the effect of Soret parameter S_r on velocity $u(1)$ when $m1 = m2 = -1$. It is noticed that with an increase in the Soret parameter when the frequency λ and the free convection $G1$,$G2$ parameters are constants, the velocity remains the same up to $y = 0.25$, increases up to $y = 0.70$ and then decreases. (curves I, II, III) and (curves VII, VIII, IX). When the frequency or free convection parameters increases with constant Soret parameter S_r, it is observed that the velocity increases to a certain point $y = 0.25$, decreases between $y = 0.25$ and $y = 0.70$, then increases (curves I and IV, II and V, III and VI) or (curves I and VII, II and VIII, III and IX).

The behaviour of the fluid velocity v (1) perpendicular to the channel is discussed in Figures 24–29. From Figure 24 it is noticed that when there is an increase in the heat source parameter α, the velocity v (1) profile decreases with constant free convection $G1$ and frequency λ parameters (curves I, II, III) and (curves VII, VIII, IX). It is also observed that with varying free convection $G1$ or frequency λ parameter, there is an increase in velocity v (1) profile when the heat source parameter

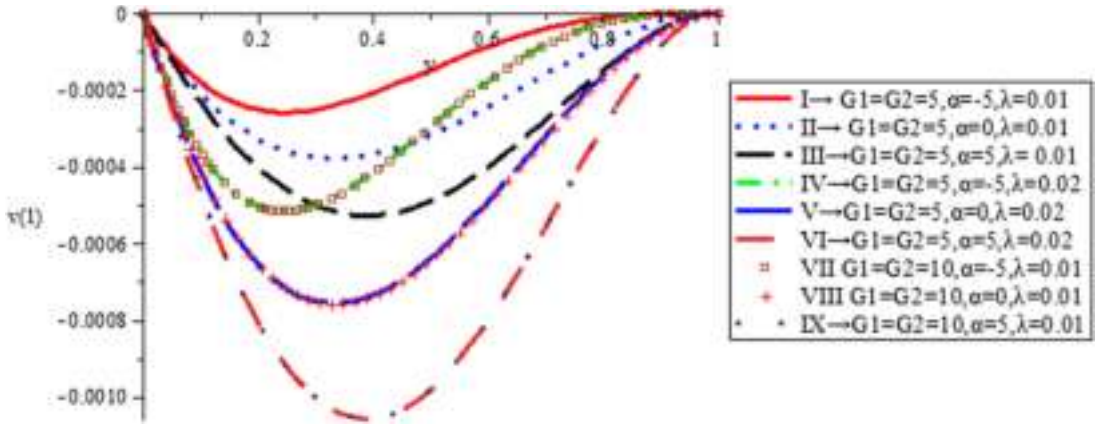

Figure 25. First-order velocity $v(1)$ profile, $m1 = m2 = -1$, $P_r = 0.71$, $S_r = 2$, $\gamma = 4$, $S_c = 0.60$, $D_u = 0.60$ and $H = 3.0$.

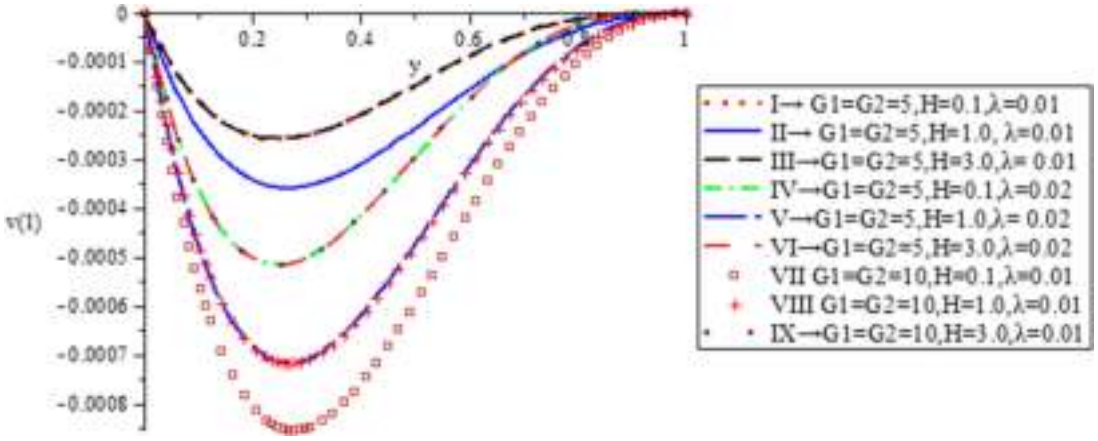

Figure 26. First-order velocity $v(1)$ profile, $m1 = m2 = -1$, $P_r = 0.71$, $S_r = 2$, $\gamma = 4$, $S_c = 0.60$, $D_u = 0.60$ and $\alpha = -5$.

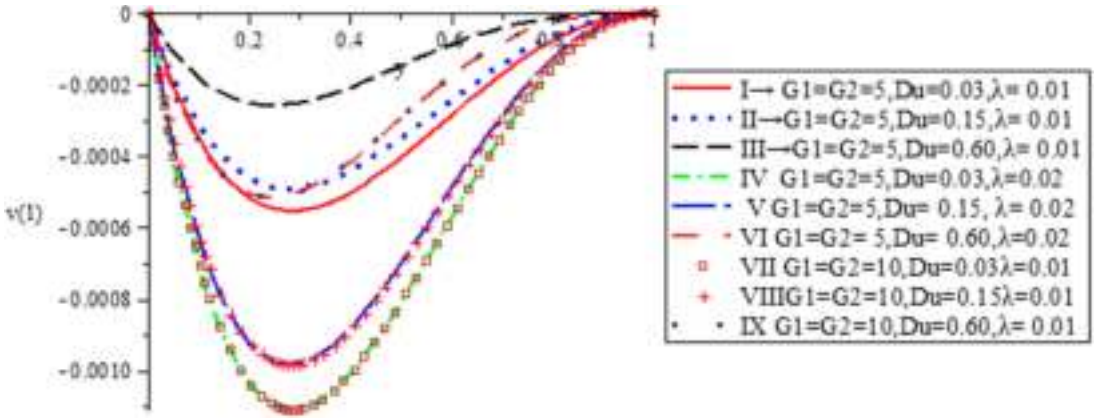

Figure 27. First-order velocity $v(1)$ profile, $m1 = m2 = -1$, $P_r = 0.71$, $S_r = 2$, $\gamma = 4$, $S_c = 0.60$, $H = 3.0$ and $\alpha = -5$.

$\alpha < 0$ (curves I, IV) and (curves I, VII) and a decrease when $\alpha \geq 0$ (curves II and V, III and VI) and (curves II and VIII, III and IX).

Figure 25 shows the effect of the embedded parameters on the fluid velocity v (1). It is clearly seen that with an increase in heat source parameter α, there is a decrease in velocity v (1) when the free convection $G1$,$G2$ and frequency λ are kept constant (curves I, II, III) and (curves VII, VIII, IX). We also realized that the velocity v (1) decreases with constant heat source parameter α, when there is an increase in free convection $G1$,$G2$ or frequency λ parameters (curves I and IV, II and V, III and VI) and (curves I and VII, II and VIII, III and IX).

The effect of MHD parameter H on the fluid velocity v (1) is as shown in Figure 26. It is observed that there is a decrease in velocity v (1) when the MHD parameter increases from $H = 0.1$ to $H = 1.0$ with constant free convection $G1$,$G2$ and frequency λ parameters (curves I and II) and (curves VII and VIII). There is also a decrease in velocity v (1) profile when there is an increase in MHD parameter from $H = 1.0$ to $H = 3.0$ (curves II and III) and (curves VIII and IX). It is, moreover, clearly seen from the

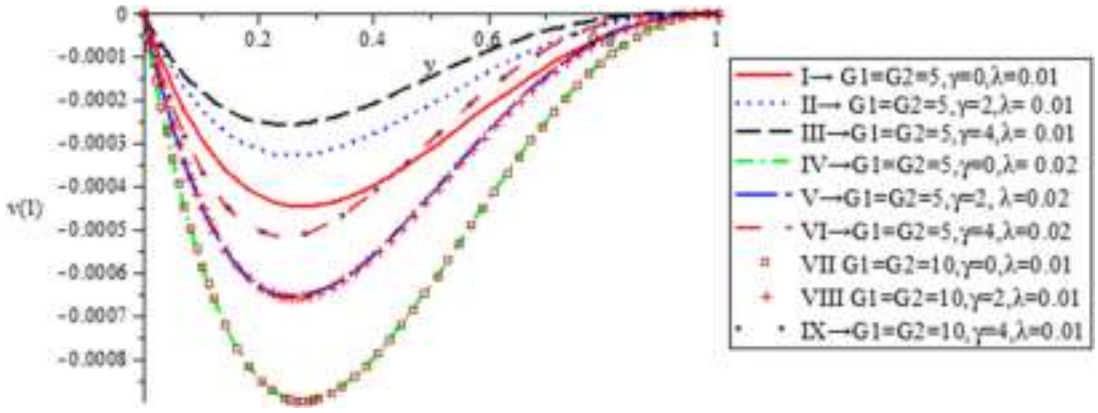

Figure 28. First-order velocity $v(1)$ profile, $m1 = m2 = -1$, $P_r = 0.71$, $S_r = 2$, $D_u = 0.60$, $S_c = 0.60$, $H = 3.0$ and $\alpha = -5$.

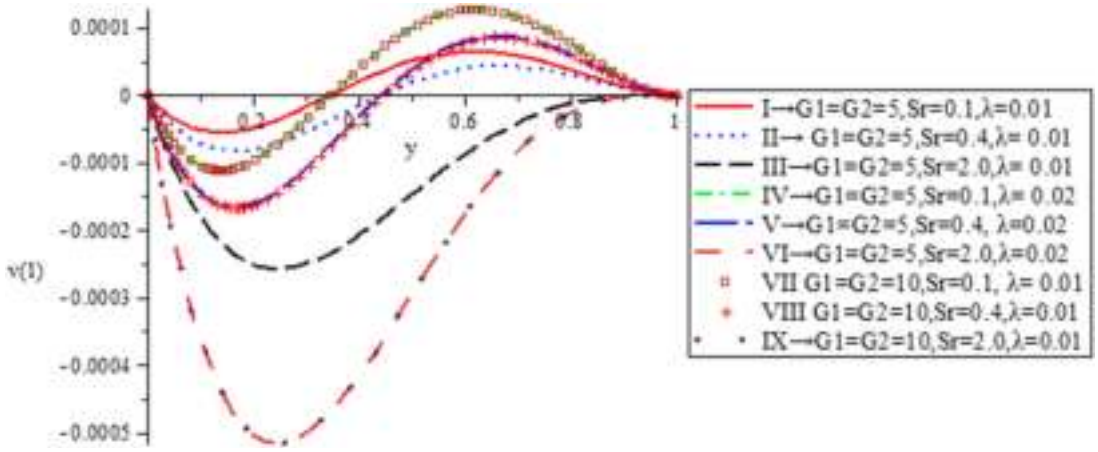

Figure 29. First-order velocity $v(1)$ profile, $m1 = m2 = -1$, $P_r = 0.71$, $\gamma = 4$, $D_u = 0.60$, $S_c = 0.60$, $H = 3.0$ and $\alpha = -5$.

figure that when there is an increase in the free convection parameters $G1$,$G2$ or frequency λ parameters, there is a decrease in velocity v (1) profiles with constant MHD parameter H (curves I and IV, II and V, III and VI) and (curves I and VII, II and VIII, III and IX).

Figure 27 reveals the effect of Dufour parameter D_u on the fluid velocity v (1) profiles. From curves (I, II III) and curves (VII, VIII, IX) of the figure, it is noticed that with increase in Dufour parameter, there is an increase in velocity v (1) profiles when the free convection parameters $G1$,$G2$ and frequency λ parameters are constant. But with an increase in frequency parameter λ or free convection parameters $G1$,$G2$, it is clearly seen that the velocity v (1) profiles decrease for a fixed value of Dufour parameter (curves I and IV, II and V, III and VI) or (curves I and VII, II and VIII, III and IX).

Figure 28 illustrates the effect of chemical reaction parameter γ on the fluid velocity v (1) profiles. It is observed from the figure that the effects of the chemical reaction parameter on the fluid velocity v (1) profile are the same as those of Dufour parameter D_u in Figure 27.

Figure 29 presents the effects of Soret parameter S_r on the fluid velocity v (1)profile. We realized from the figure that with an increase in the Soret parameter, the velocity v (1) profile decreases across the channel width when the free convection parameters $G1$,$G2$ and frequency λ parameters are constant (curves I, II, III) and (curves VII, VIII, IX). An increase in each of $G1$ and $G2$ and λ leads to a decrease to a particular point of y and then an increase when there is an increase in Soret parameter from $S_r = 0.1$ to$S_r = 0.4$ (curves I and IV, II and V) and (curves I and VII, II and VIII). A decrease in velocity $v(1)$ across the channel width is experienced when there is an increase in Soret parameter from $h = 0.4$ to $S_r = 2.0$ (curves III and VI) and (curves III and IX).

4.2.2. Temperature profiles

Figures 30–33 depict the behaviour of the fluid temperature $\theta(1)$ profiles. Figure 30 describes the effect of MHD parameter H on the fluid temperature $\theta(1)$ profile. It is noticed that with an increase in H, there is a decrease in the fluid temperature $\theta(1)$ profile when free convection parameters $G1$,$G2$ and frequency parameters λ are kept constant, (curves I, II, III) and (curves VII, VIII, IX). We also observed that when there is an increase in free convection parameters $G1$,$G2$ with parameters λ, α, H remaining constant or an increase in frequency parameter λ with parameters $\alpha, H, G1, G2$ being constant, there is a decrease in fluid temperature $\theta(1)$ profiles (curves I and VII, II and VIII, III and IX) or (curves I and IV, II and V, III and VI).

Figure 31 and 32 show the effects of Dufour parameter D_u and chemical reaction (γ) respectively on the fluid temperature $\theta(1)$ profiles. It is observed that their

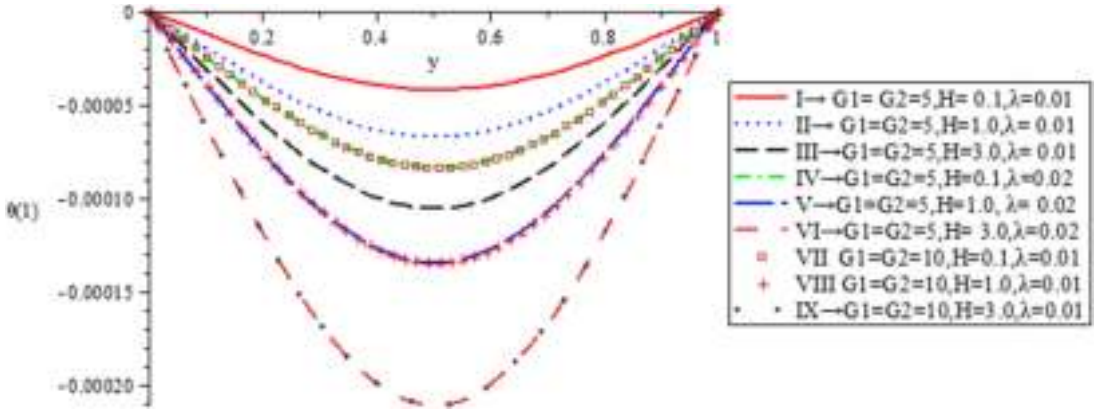

Figure 30. First-order temperature $\theta(1)$ profile, $m1 = m2 = -1$, $P_r = 0.71$, $S_r = 2$, $\gamma = 4$, $D_u = 0.60$ and $\alpha = -5$.

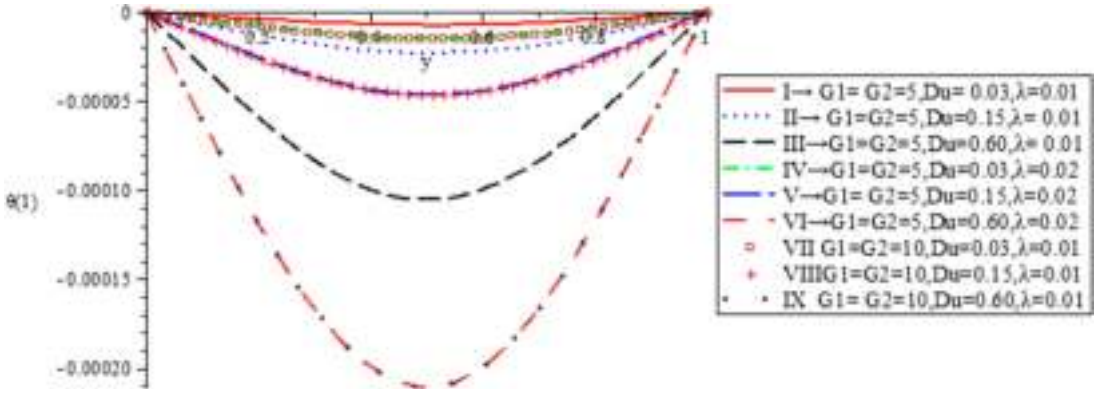

Figure 31. First-order temperature $\theta(1)$ profile, $m1 = m2 = -1$, $P_r = 0.71$, $S_r = 2$, $\gamma = 4$, $H = 3.0$, $S_c = 0.60$ and $\alpha = -5$.

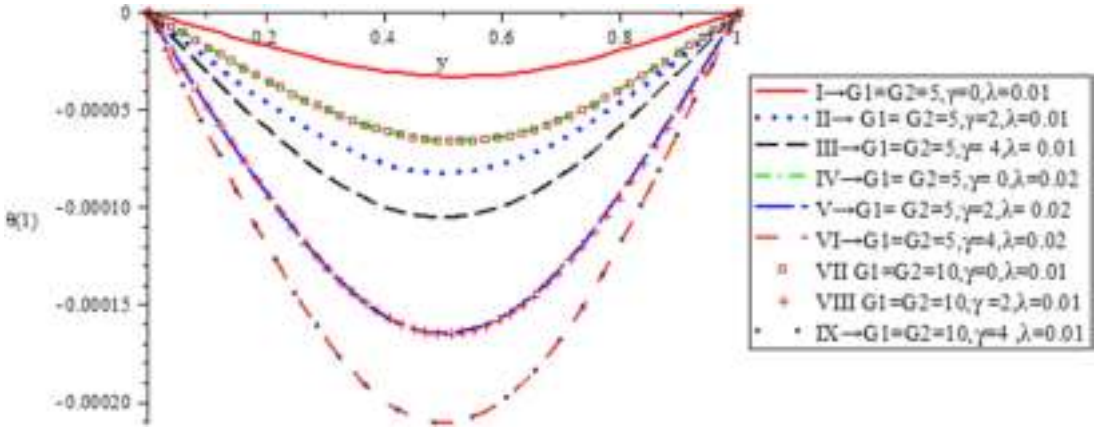

Figure 32. First-order temperature $\theta(1)$ profile, $m1 = m2 = -1$, $P_r = 0.71$, $D_u = 0.60$, $S_r = 2$, $S_c = 0.60$, $H = 3.0$ and $\alpha = -5$.

effects on fluid temperature remain the same as the effect of MHD parameter H in Figure 30.

Figure 33 reveals the effect of Soret parameter S_r on the fluid temperature $\theta(1)$ profiles. It is clearly seen from the figure that with an increase in S_r, there is an increase in temperature $\theta(1)$ profile of the fluid, when the free convection parameters $G1$,$G2$ and frequency λ are kept constant (curves I, II, III) and (curves VII, VIII, IX). However, a decrease in the fluid temperature $\theta(1)$ is observed, when there is an increase in the free convection parameters $G1$,$G2$ or frequency λ with constant Soret parameter S_r (curves I and IV, II and V, III and VI) and (curves I and VII, II and VIII, III and IX).

4.2.3. Concentration profiles

The behaviour of the fluid concentration c (1)profiles is depicted in Figures 34–37. It is observed from Figure 34 that an increase in heat source parameter α, leads to a decrease in fluid concentration c (1) profiles when free convection parameters $G1$,$G2$ and frequency parameter λ are constant (curves I, II, III) and (curves VII, VIII, IX). On keeping heat source parameter α constant and increasing the free convection parameters $G1$,$G2$ or frequency parameter λ, a decrease in fluid concentration c (1) profiles is noticed (curves I and VII, II and VIII, III and IX) or (curves I and IV, II and V, III and VI).

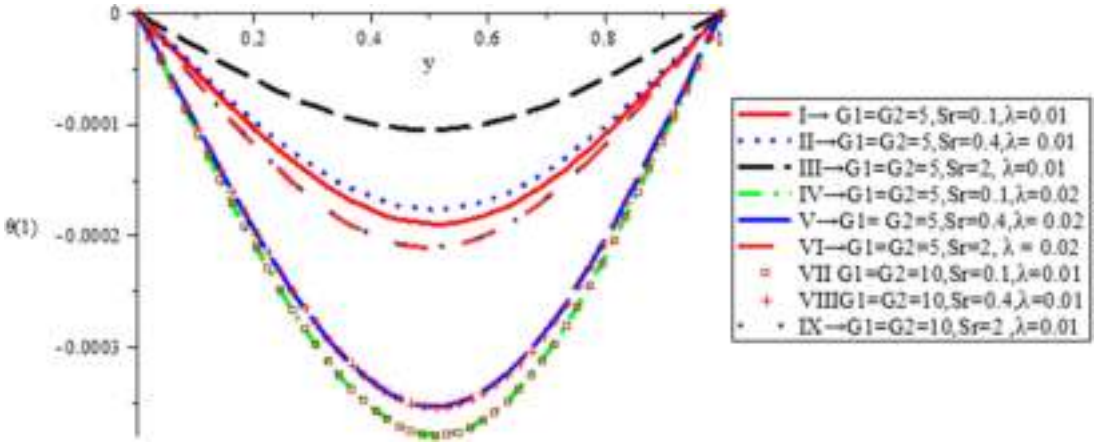

Figure 33. First-order temperature $\theta(1)$ profile, $m1 = m2 = -1$, $P_r = 0.71$, $D_u = 0.60$, $\gamma = 4$, $H = 3.0$, $S_c = 0.60$ and $\alpha = -5$.

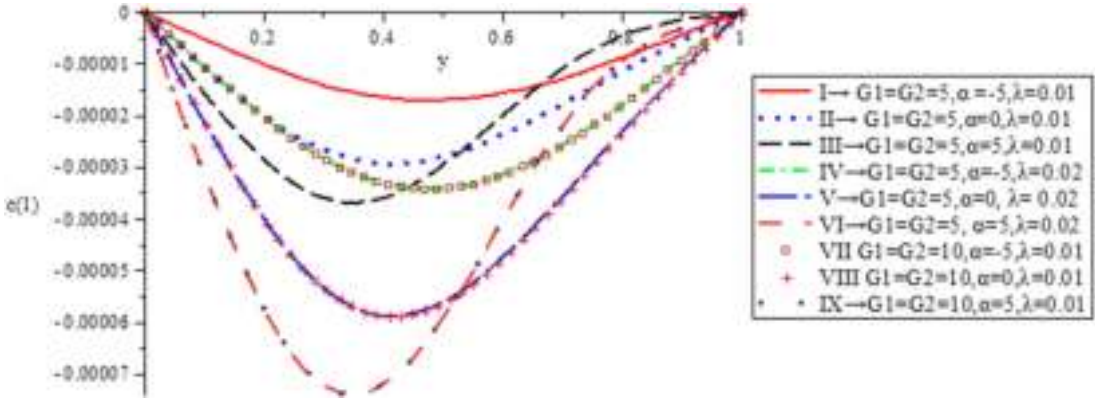

Figure 34. First-order concentration $c(1)$ profile, $m1 = m2 = -1$, $S_c = 0.60$, $S_r = 2$, $\gamma = 4$, $D_u = 0.60$, $P_r = 0.71$ and $H = 3.0$.

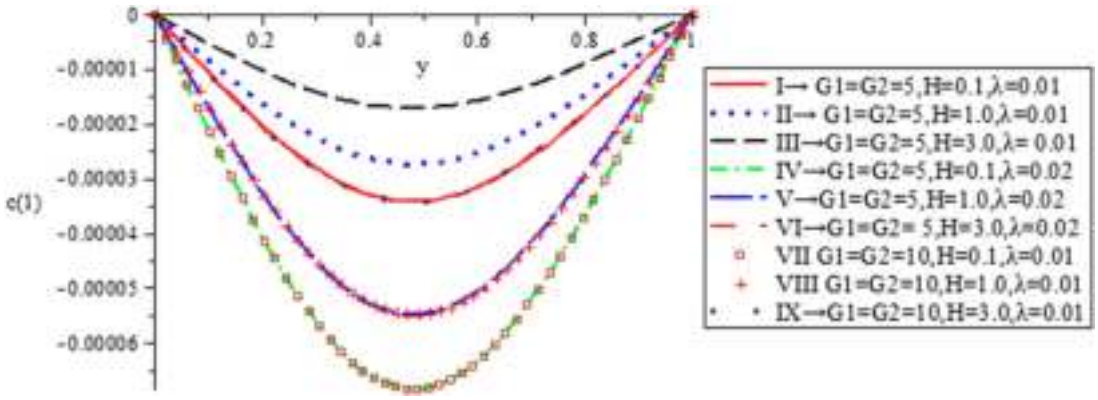

Figure 35. First-order concentration $c(1)$ profile, $m1 = m2 = -1$, $S_c = 0.60$, $P_r = 0.71$, $S_r = 2$, $\gamma = 4$, $D_u = 0.60$ and $\alpha = -5$.

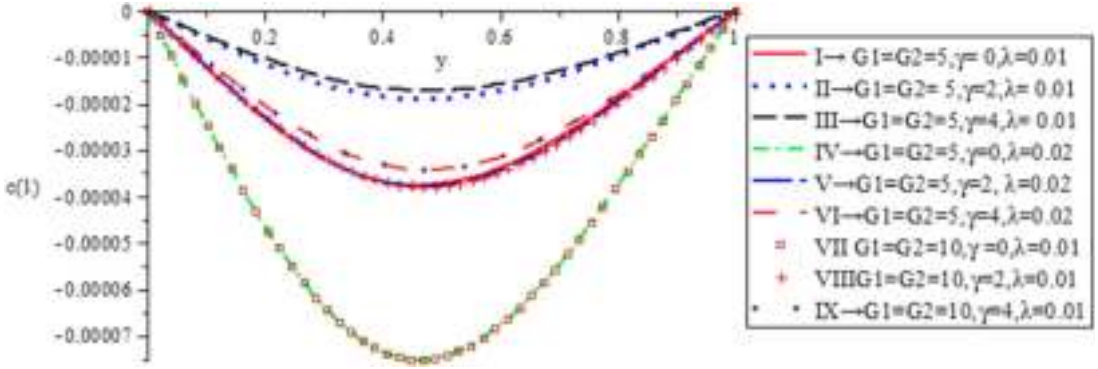

Figure 36. First-order concentration $c(1)$ profile, $m1 = m2 = -1$, $S_c = 0.60$, $P_r = 0.71$, $S_r = 2$, $D_u = 0.60$,$H = 3.0$ and $\alpha = -5$.

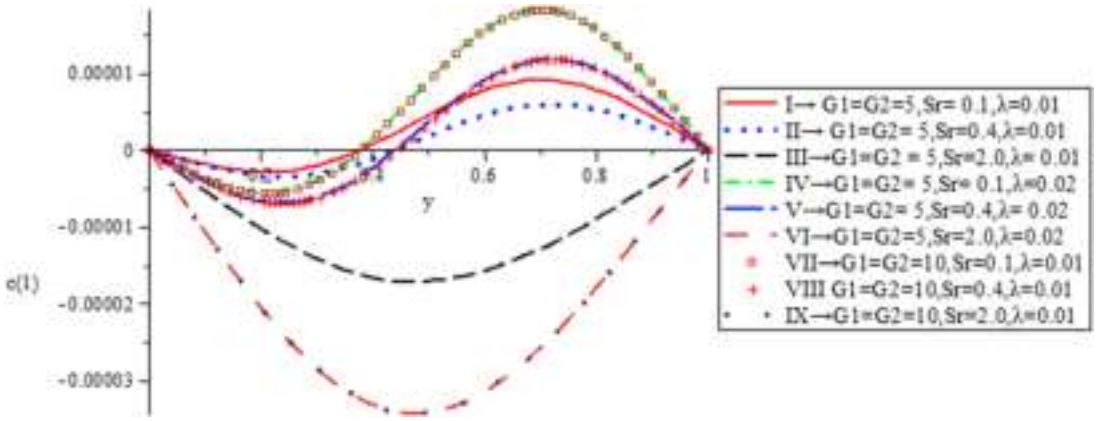

Figure 37. First-order concentration $c(1)$ profile, $m1 = m2 = -1$, $S_c = 0.60$, $P_r = 0.71$, $\gamma = 4$, $D_u = 0.60$, $H = 3.0$ and $\alpha = -5$

Figure 35 illustrates the effect of MHD parameter H on the fluid concentration c (1)profiles. It is clearly seen that with an increase in MHD parameter H, there is an increase in fluid concentration c (1) profiles when the free convection $G1$,$G2$ and frequency λ are kept constant (curves I, II, III) and (curves VII, VIII, IX). The reverse is the case when there is an increase in free convection parameters $G1$,$G2$ or frequency parameter λ with constant MHD parameter H (curves I and IV, II and V, III and VI) and (curves I and VII, II and VIII, III and IX).

Figure 36 deals with the effect of chemical reaction parameter γ on the fluid concentration c (1) profiles. It is observed that the behaviour remains the same as that of the effect of MHD in Figure 35

The effect of Soret parameter S_r on the fluid concentration c (1) profiles is shown in Figure 37. It is noticed that the fluid concentration c (1) profile decreases across the channel width, with an increase in Soret parameter when free convection parameters $G1$,$G2$ and frequency λ are constant (curves I, II, III) and (curves VII, VIII, IX). It is also observed that there is a decrease in fluid concentration c (1) profile up to a particular point on the width of the channel and then an increase, with an increase in frequency parameter λ or free convection parameters $G1$,$G2$ when $S_r = 0.1$ and $S_r = 0.4$ (curves I and IV, II and V) or (curves I and VII, II and VIII). While a decrease in fluid concentration $c(1)$ profile is observed when $S_r = 2.0$ for an increase in frequency parameter λ or free convection parameters $G1$,$G2$ (curves III and VI) or (curves III and IX).

5. Conclusions

A numerical study has been conducted on free convective heat and mass transfer of an incompressible electrically conducting fluid in a finitely long vertical wavy channel, considering Soret, Dufour and chemical reaction effects in the presence of constant heat source or sink. Employing the perturbation technique, the solutions of the dimensionless governing equations are assumed to be of a mean part and disturbance (contribution from the waviness of the wall) part and are evaluated numerically using the Adomian decomposition method with MAPLE 14 software.

Numerical results of the fluid flow are presented for different physical parameters and are shown by means of graphs. From the previous results and discussion, the numerical observations are as follows:

(i) When $H = 0, D_u = 0, S_r = 0$ and $\gamma = 0$, the numerical values are the same with that of Vajravelu and Sastri [1] and Fasogbon [2] for $u_0, \theta_0, c_0, u_1, v_1, \theta_1$ and c_1 for different values of $\alpha, G1, G2, m1, m2$ and λ which confirm the validity of our numerical simulation.

(ii) An increase in the magnetic field parameter H, chemical reaction parameter γ and Dufour number D_u considerably reduced the mean velocity, but get enhanced due to increase in Soret number S_r.

(iii) A rise in the Soret number S_r depreciates the mean temperature profiles of the flow while an increase in Dufour number D_u and chemical reaction parameter γ enhanced it.

(iv) Heat source/sink parameter α and chemical reaction parameter γ have tendency to decrease the mean concentration profile and Soret number S_r accelerates it.

(v) It is found, in general, that $G1$,$G2$,$m1$,$m2$ and α strongly enhanced the mean velocity, temperature and concentration.

(vi) On fixing $G1$,$G2$,$m1$,$m2$ and α, the effects of λ, H, D_u, γ and S_r on the fluid velocity u_1 are qualitatively similar.

(vii) Changes in the value of α, H and S_r reduced the fluid velocity v_1 perpendicular to the channel length when $G1$,$G2$ and λ are fixed but this trend is reversed in the case of D_u and γ.

(viii) Increase in the value of H, D_u and γ diminished the fluid temperature θ_1 considerably when $G1$,$G2$ and λ are fixed but Soret number S_r has tendency to increase it.

(ix) The effect of an increase in the Soret number S_r and heat source/sink parameter α suppressed the

concentration $c1$ when $G1$,$G2$ and λ are fixed. This trend is reversed in the effect of H and γ.

(x) It is evident that the perturbed quantities u_1, v_1, θ_1 and $c1$ are affected significantly by the free convection parameters $G1$,$G2$, the heat source/sink parameter α and the wavelength parameter λ.

(xi) The flow pattern of the perturbed part leads to non-uniqueness in the exhibited wave-like trend along the y-direction. That is, we record the qualitative differences in the behaviour of the various flows which show clearly the effects of the channel under consideration.

NOMENCLATURE

C'	species concentration at any point in the fluid
c	dimensionless concentration
C_s	concentration susceptibility
C_w	species concentration at the wavy wall
c_0	zeroth-order concentration
c_1	first-order concentration
C_p	specific heat at constant pressure
C_s'	concentration of the fluid in static condition
d	distance between the walls
D_m	mass diffusion coefficient
D_u	diffusion-thermo parameter
$G1$	thermal Grashof number
$G2$	mass Grashof number
$m1$	wall temperature ratio
$m2$	wall concentration ratio
g_x	acceleration due to gravity in x-direction
K_T	fluid thermal-diffusion ratio
k_1	constant rate of chemical reaction
K	thermal conductivity
T'	dimensional temperature of the fluid
T_s	fluid temperature in static condition
T_w	wavy wall temperature
T_1	temperature of the flat wall
T_m	mean fluid temperature
P'	dimensional fluid pressure
p	dimensionless fluid pressure
P_r	Prandtl number
Q	the constant heat source/sink
S_c	Schmidt number
S_r	thermal-diffusion parameter
H	magnetic field parameter
k	wave number
ρ	fluid density
σ	electrical conductivity
β_0	externally imposed magnetic field
β	magnetic field strength
β_c	coefficient of concentration expansion
β_T	coefficient of thermal expansion
α	Heat source or sink parameter
U', V'	velocity components along the (X,Y) axes
u,v	dimensionless velocity
u_0	dimensionless zeroth-order velocity
u_1, v_1	dimensionless first-order velocity
X', Y'	dimensional coordinate system
x,y	dimensionless coordinate system
ϵ^*	irregular wall amplitude
ϵ	dimensionless amplitude
λ	dimensionless wave length of the irregular wall
μ	dynamic viscosity
ν	fluid kinematic viscosity
θ	dimensionless temperature of the fluid
θ_0	dimensionless zeroth-order temperature profiles
θ_1	dimensionless first-order temperature profiles
ψ_1	stream function
γ	chemical reaction parameter

Disclosure statement

No potential conflict of interest was reported by the authors.

ORCID

J.A. Gbadeyan http://orcid.org/0000-0003-2704-3791
P.F. Fasogbon http://orcid.org/0000-0001-8541-877X
J.U. Abubakar http://orcid.org/0000-0002-2079-5731

References

[1] Vajravelu K, Sastri KS. Free convective heat transfer in a viscous incompressible fluid confined between a long vertical wavy wall and a parallel flat wall. J Fluid Mech. 1978;86(2):365–383.

[2] Fasogbon PF. Analytical studies of heat and mass transfer by convection in a two dimensional irregular channel. Int J Appl Math Mech. 2010;6(4):17–37.

[3] Davika B, Satya Narayana PV, Venkataramana S. Chemical reaction effects on MHD free convection flow in an irregular channel with porous medium. Int J Math Arch. 2013;4(4):282–295.

[4] Dada MS, Disu AB. Heat transfer with radiation and temperature dependent heat source in MHD free convection flow in a porous medium between two vertical wavy walls. J Nigeria Math Soc. 2014. http://dx.doi.org/10.1016/j.jnnms2014.12.001.

[5] Fasogbon PF, Omolehin JO. Radiation effect on natural convection in spirally enhanced channel. leJEMTA. 2008;3(1):1–28.

[6] Abubakar JU. Natural convective flow and heat transfer in a viscous incompressible fluid with slip confined within spirally enhanced channel [Unpublished Ph.D thesis]. University of Ilorin; 2014

[7] Kumar H. Heat transfer with radiation and temperature dependent heat source in MHD free convection flow confined between two vertical wavy walls. Int J Appl Math Mech. 2011;7(2):77–103.

[8] Kafoussias NG, Williams EW. Thermal-diffusion and diffusion-thermo effects on mixed free forced convective and mass transfer boundary layer flow with temperature dependent viscosity. Int J Eng Sci. 1995;33:1369–1384.

[9] Gbadeyan JA, Idowu AS, Ogunsanya AW, et al. Heat and mass transfer for Soret and Dufour's effect on mixed convection boundary layer flow over a stretching vertical surface in a porous medium filled with a viscoelastic fluid in the presence of magnetic field. Global J Sci Front Res. 2011;11(8):97–114.

[10] Makinde OD, Olanrewaju PO. Unsteady mixed convection with Soret and Dufour effects past a porous plate moving through a binary mixture of chemically reacting fluid. Chem Eng Commun. 2011;198:920–938.
[11] Olanrewaju PO, Gbadeyan JA. Effect of Soret Dufour, Chemical reaction, thermal radiation and volumetric heat generation/absorption on mixed convection stagnation point flow on an iso-thermal vertical plate in porous media. Pac J Sci Tech. 2011;12(2):234–245.
[12] Alam MS, Ferdows M, Ota M, et al. Dufour and Soret effect of steady free convection and mass transfer flow past a semi-infinite vertical porous plate in a porous medium. Int J Appl Mech Eng. 2006;11:535–545.
[13] Olanrewaju PO, Adeniyan A, Sanmi FA. Soret and Dufour effects on hydromagnetic free convection flow with heat and mass transfer past a porous plate in the presence of chemical reaction and thermal radiation. Far East J Appl Math. 2013;80(1):41–66.
[14] Olanrewaju PO, Makinde OD. Effect of thermal diffusion and diffusion thermo on chemically reacting MHD boundary layer flow of heat and mass transfer past a moving vertical plate with suction/injection. Arab J Sci Eng. 2011. doi:1007/S13369-011-0143-8.
[15] Das UN, Ahmed N. Free convective MHD flow and heat transfer in a viscous incompressible fluid confined between a long vertical wavy wall and a parallel flat wall. Indian J Pure Math. 1992;23(4):295–304.
[16] Disu AB, Dada MS. Raynold's model viscosity on radiative MHD flow in a porous medium between two vertical wavy walls. J Taibah Univ Sci. 2017;11:548–565.
[17] Loganathan P, Iranian D, Ganesan P. Effect of chemical reaction on unsteady free convective and mass transfer flow past a vertical plate with variable viscosity and thermal conductivity. Eur J Sci Res. 2011;59(31):403–416.
[18] Chamkha AJ, Aly AM, Mansour MA. Natural convective power-law fluid flow past a vertical plate embedded in a non-darcian porous medium in the presence of a homogeneous chemical reacting non-linear analysis. Model Control. 2010;15(2):139–154.
[19] Chen W, Lu Z. An algorithm for Adomian decomposition method. Appl Math Comput. 2004;159:221–235.